



**HAL**  
open science

## Review on Otological Robotic Systems: Toward Microrobot-Assisted Cholesteatoma Surgery

Bassem Dahroug, Brahim Tamadazte, Stefan Weber, Laurent Tavernier,  
Nicolas Andreff

► **To cite this version:**

Bassem Dahroug, Brahim Tamadazte, Stefan Weber, Laurent Tavernier, Nicolas Andreff. Review on Otological Robotic Systems: Toward Microrobot-Assisted Cholesteatoma Surgery. *IEEE Reviews in Biomedical Engineering*, 2018, 11, pp.125-142. 10.1109/RBME.2018.2810605 . hal-04249811

**HAL Id: hal-04249811**

**<https://hal.science/hal-04249811v1>**

Submitted on 19 Oct 2023

**HAL** is a multi-disciplinary open access archive for the deposit and dissemination of scientific research documents, whether they are published or not. The documents may come from teaching and research institutions in France or abroad, or from public or private research centers.

L'archive ouverte pluridisciplinaire **HAL**, est destinée au dépôt et à la diffusion de documents scientifiques de niveau recherche, publiés ou non, émanant des établissements d'enseignement et de recherche français ou étrangers, des laboratoires publics ou privés.

# Review on Otological Robotic Systems: Toward Micro-Robot Assisted Cholesteatoma Surgery

Bassem Dahroug<sup>1</sup>, Brahim Tamadazte<sup>1</sup>, Stefan Weber<sup>2</sup>, Laurent Tavernier<sup>3</sup>, and Nicolas Andreff<sup>1</sup>

## Abstract

Otologic surgical procedures tend over time to become minimally invasive due to the development of medicine, micro-techniques and robotics. This trend is expected to reduce the patient's recovery time and to improve the accuracy in diagnosis and treatment. One of the most challenging difficulties that face such techniques are precise control of the instrument and supply of an ergonomic system to the surgeon. The objective of this literature review is to present requirements and guidelines for a surgical robotic system dedicated to the middle ear surgery. This review is particularly focused on cholesteatoma surgery (diagnosis and surgical tools) which is one of the most frequent pathologies that urge for an enhanced treatment. The paper also presents the current robotic systems which are implemented for otologic applications.

## Index Terms

Middle ear surgery, cholesteatoma, medical robotics, micro-robotics, image-guided surgery.

## Contents

I	Introduction	2
---	--------------	---

<sup>1</sup> are with FEMTO-ST Institute, AS2M department, Univ. Bourgogne Franche-Comté/CNRS/ENSMM, 24 Rue Alain Savary, 25000 Besançon, France. brahim.tamadazte@femto-st.fr

<sup>2</sup> is with ARTORG Center for Biomedical Engineering, Univ. of Bern, Bern, Switzerland. stefan.weber@artorg.unibe.ch

<sup>3</sup> is with Univ. Hospital of Besançon, Université Bourgogne Franche-Comé, Besançon, France ltavernier@chu-besancon.fr

This work has been supported by the Labex ACTION project (ANR-11LABX-0001-01), CoErCIVE Bourgogne Franche-Comté Regional Project, and  $\mu$ RoCS Project (ANR-17-CE19-0005-04).

II	Cholesteatoma disease	5
II-A	Ear Anatomy . . . . .	5
II-B	Definition . . . . .	6
II-C	Physiopathology, Complication and Epidemiology . . . . .	6
II-D	Diagnosis . . . . .	7
II-E	Treatment . . . . .	10
II-F	Ablation Tools . . . . .	12
III	Surgical robotic system	13
III-A	Ideal Requirements for Robot-assisted Cholesteatoma Surgery . . . . .	13
III-B	Otological surgical robotic systems . . . . .	17
III-B1	Inner ear surgery . . . . .	17
III-B2	Middle ear surgery . . . . .	23
IV	Guidelines for the required micro-robotic assisted cholesteatoma surgery	26
IV-A	Clinical . . . . .	27
IV-B	Robotic Structure and Computer-Assisted Surgery . . . . .	28
IV-C	Safety and risk analysis . . . . .	30
IV-D	Targeted Robotic Concept for Middle Ear Surgery . . . . .	31
V	Conclusion	31
	References	33

## I. Introduction

Cholesteatoma consists of squamous epithelium that is trapped within the skull base [1], and which can erode and destroy important structures within the temporal bone, especially the middle ear structures (e.g., the ossicles as depicted in Fig. 1). The only treatment in the current medical practice is a surgical intervention, and its efficiency depends on the surgeon skills. In addition, post-operative complications may occur, such as facial nerve damage, total neurosensory hearing loss, residual tympanic membrane perforation and balance disturbance.

<sup>1</sup>Image of Cholesteatoma evolution [online]. <http://entkidsadults.com/ent-diagnosis/ear-nose-throat/cholesteatoma/>

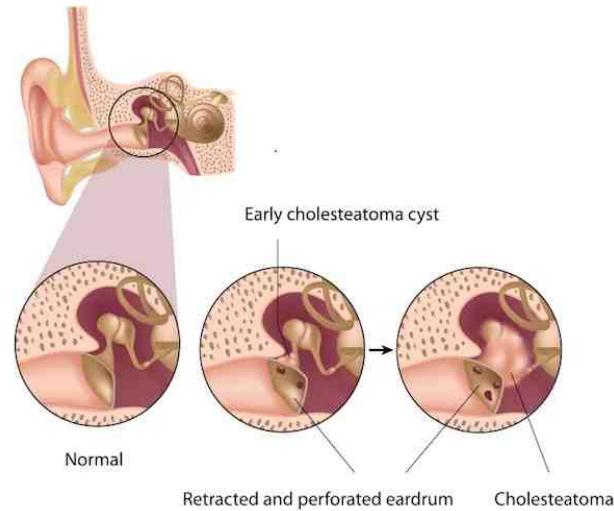


Fig. 1. Description of different parts of auditory system and Cholesteatoma progress over time <sup>1</sup>.

Depending on the surgical procedure, approximately ten to thirty percent of cholesteatoma operations are unsuccessful with some residual or recurrent cholesteatoma cells [1] [2]. Recurrent cholesteatoma means that the disease grows again after the ablation process, while residual cholesteatoma refers to the cells that have been left behind by the surgeon. In both cases, an MRI (Magnetic Resonance Imaging) revision is performed (two to three times with an interval of six months between each examination). This revision has the objectives: i) to visualize and observe the evolution of the cholesteatoma cells aggregation, ii) to determine whether it is necessary to perform a secondary procedure (also known as "second-look procedure") or not.

In fact, prior to the use of MRI and CT (Computer Tomography), the incidence of secondary procedures was very high (almost all patients underwent a second surgery), while the use of medical imaging has reduced the incidence to thirty percent. However, the limited access to the middle ear cavity, as well as the difficulties to detect the disease with enough accuracy prevents from reducing the prevalence of secondary interventions. Consequently, there is a clinical need to reduce this percentage even more, or to completely avoid it, and an opportunity to do so thanks to a high added-value robotic system, relying on advanced mechatronics and innovative image-guided control strategies. Such a robotic system should provide the surgeon with super-human capabilities: increased accuracy, real-time tool monitoring, data logging, traceability and ergonomic. Such a system should also yield reduced invasiveness.

Over the previous three decades, surgical robotics has become an active research branch by providing solutions for a wide range of clinical problems [3]. More recently, the development of

miniaturization methods has and will contribute to the advancement of micro- and nano-robots [4] [5] [6] [7] which should improve both the biopsy and the therapy of auditory system disorders and diseases.

Improving the effectiveness of cholesteatoma removal in addition to reducing the risk of anatomical lesions by increasing the accuracy and repeatability of the treatment has the potential to improve surgical outcomes and ultimately patients benefit. Further, specific targeting of diseased tissues with the aid of image-guided and bendable surgical robotics would improve access capabilities, and thus reduce the need for large incisions and bone tissues removal, resulting in reductions in invasiveness, patient recovery time, operation time and costs. Furthermore, the auditory system size and its location in the skull prevents from using conventional surgical robots. As a consequence, an unprecedented microrobot-assisted otological system must be invented.

Robot-assisted cholesteatoma surgery has not yet been explored, despite the evident benefits and the trend towards robotic assistance. Within this article, a review of the otologic robotic systems, medical imaging modalities, and interventional tools are presented towards the realization of a system suitable for cholesteatoma surgery. This review has also the objective to be a source of inspiration for a newcomer to the field of otological surgery, and those concerned in cholesteatoma treatment as engineers, scientists or surgeons. It also aims at providing an exhaustive description of the scattered bits of investigation related to robot-assisted cholesteatoma surgery. It faces the challenge to be readable both by an otorhinolaryngologist and by a roboticist. May each of them forgive us the simplifications necessary to the other one's understanding and interest. Thus, Section II provides the clinical information to the readers who are not familiar with the cholesteatoma disease. It deals with the cholesteatoma pathology, its complications, epidemiologic issues, diagnostic imaging systems, and more details on the current surgical treatment, as well as the ablation tools. Section III-A presents then the ideal requirements and specifications for an ideal system without any constraints on the available technology. Afterwards, Section III-B shows the current state of otological robotics. It provides an exhaustive survey of otological robotic systems and their limitations for possible use throughout cholesteatoma surgery. At the end, Section IV discusses the presented materials. It lays down detailed technical guidelines for the future development of an efficient and reliable micro-robotic system for cholesteatoma removal. This last section also highlights some tracks to be investigated.

## II. Cholesteatoma disease

### A. Ear Anatomy

The auditory system is a delicate mechanism and it consists typically of three parts: external ear, middle ear and inner ear. It is sustained in the skull base, more precisely in the temporal bone and the mastoid portion which is formed of bone filled with air cells [8].

The outer ear is the external portion which consists of the pinna (auricle) and the external ear canal (auditory meatus). This canal length is about  $25\text{mm}$  and its diameter varies from  $5\text{mm}$  to  $10\text{mm}$  [9] (Fig. 2). The external ear gathers and focuses the sound waves to make the tympanic membrane vibrate. These vibrations are transmitted from the middle ear to the inner ear due to the motion of three tiny bones (i.e., the ossicles: malleus, incus and stapes).

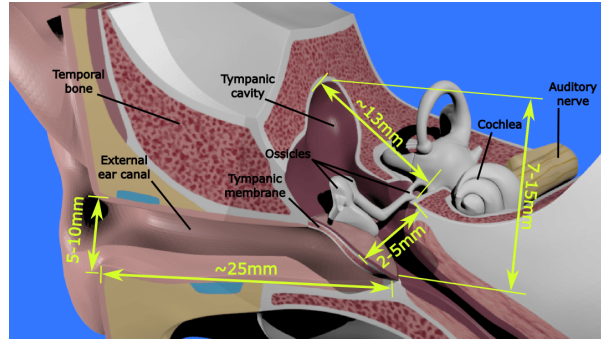


Fig. 2. Dimensions of different parts of auditory system.

The inner ear is composed of the cochlea and the three semi-circular canals, which are the sensory receptors of hearing and balancing, respectively. The middle ear consists mainly of the tympanic membrane and the tympanic cavity that shields the ossicles. This cavity has an irregular parallelepiped form [9], where its length is around  $13\text{mm}$  (from front to back), its height has a maximum variation from  $7\text{mm}$  to  $15\text{mm}$  (from top to bottom), and the width varies from  $2\text{mm}$  to  $5\text{mm}$  (from left to right), see Fig. 2. The volume of this cavity varies from one person to another, which also increases during the individual growth periods approximately from  $452\text{mm}^3$  for an infant to  $640\text{mm}^3$  for an adult [10].

To improve the surgeon capabilities within this millimetric confined workspace, a surgical micro-robot is crucial for providing dexterity and ergonomic, facilitating the access, and maximizing visibility and manoeuvrability during the surgical intervention.

## B. Definition

Cholesteatoma consists of squamous epithelium that erodes and destroys structures within the temporal bone [11]. It occurs when epithelial cells produce keratin<sup>2</sup> in the middle ear cavity. This cavity gathers the tympanic cavity and the pneumatic portions of the temporal bone. Cholesteatoma is usually classified into three types: congenital, primary acquired and secondary acquired cholesteatoma [1]. Acquired cholesteatoma is related to an alteration of the tympanic membrane. The primary acquired cholesteatoma is usually limited to the fragile top part of the tympanic membrane (i.e., the pars flaccida) (Fig. 3(a)). The secondary acquired cholesteatoma appears after a trauma of the tympanic membrane or fracture of the temporal bone. The congenital type, rarer than the acquired ones, occurs behind an intact tympanic membrane (Fig. 3(b)).

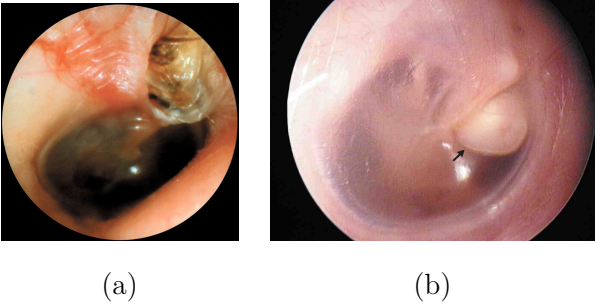


Fig. 3. (a) Typical primary acquired cholesteatoma which destroyed the top region of the tympanic membrane [12]; (b) typical congenital cholesteatoma deep within a normal tympanic membrane<sup>4</sup>.

## C. Physiopathology, Complication and Epidemiology

The origin of cholesteatoma has been subject to extensive debates [1]. On the one hand, the origin of congenital cholesteatoma is remnants of epithelial tissues behind an intact tympanic membrane, after birth. On the other hand, there are pieces of evidence for, at least, four different mechanisms that may explain the development of acquired cholesteatoma: i) squamous metaplasia theory, ii) basal hyperplasia theory, iii) immigration or invasion theory, and iv) retraction pocket theory. Moreover, these mechanisms may be combined. The retraction pocket theory is the most widely supported. Under this theory, there is an invagination of tympanic membrane cells into the middle ear due to the Eustachian tube dysfunction, inflammation of the middle ear mucosa or both [1].

<sup>2</sup>Keratin is a tough, insoluble portion substance that is the chief structural constituent of skin, hair and nails.

<sup>4</sup>Image of congenital Cholesteatoma [online]. <http://www.nejm.org/doi/full/10.1056/NEJMicm0911270>

Cholesteatoma has a destructive nature; it expands gradually and causes complications by the erosion of adjacent bony structures. The ossicular chain is the structure which is the most frequently damaged. Thus, it leads to a conductive hearing loss. Cholesteatoma can also reach the facial nerve and thus cause a facial paralysis. On long duration, it may even cause a brain complication by perforating the skull bone portion between the middle ear and the meninges [11] [13].

Each year, around 10 new cases per 100,000 inhabitants are infected by cholesteatoma. It affects also men more than women, and children less than adults [14] [15] [16]. More important is the high incidence of residual cholesteatoma which varies from 10% to 30% percent, and it is higher in children than adults [17] [18] [2]. TABLE I shows recent French statistics from ATIH <sup>5</sup> that represent the total number of cholesteatoma interventions.

Year	H71	H95.0 (H71%)	Total (H71+H95.0)
2012	7355	766 (10.4%)	8121
2013	7214	835 (11.6%)	8049
2014	7066	770 (10.9%)	7836

TABLE I

The number of cholesteatoma interventions in France <sup>6</sup>.

#### D. Diagnosis

As far as diagnosis is concerned, an HR-CT (High-Resolution Computerized Tomography) and an MRI are widely used in the pre- and post-operative cholesteatoma assessments [19]. These methods are considered as the standard imaging techniques. Other methods are still in the research development phase, such as ultrasound imaging, fluorescence microscope and OCT (Optical Coherence Tomography) [20]. These imaging techniques provide an optical biopsy (micro-metric resolution and real-time imaging modalities) during the intra-operative phase, except to HR-CT.

Standard diagnostic imaging: On the one side, the HR-CT provides good information about the ossicles and the bony structures. On the other side, MRI is useful for characterizing soft tissue, such as cholesteatoma. However, the current clinical MRI systems cannot detect lesions smaller

<sup>5</sup>ATIH: Agence Technique de l'Informatique sur l'Hospitalisation (French healthcare database). [online] <http://www.atih.sante.fr/statistiques-par-ghm-0>

<sup>6</sup>where H71: the number of patients whose had a first cholesteatoma surgery, H95.0: the number of patients whose had another intervention to remove the residual cholesteatoma, and H71+H95.0: the total number of cholesteatoma interventions in each year.



than  $3mm$ , and are not considered as a valid alternative to the second-look operation [21] [12] [19] since the residual cholesteatoma size is often less than  $3mm$ . Consequently, the diagnosis of residual cholesteatoma is often difficult which explains the need for a second-look in too many cases. This also urge for developing intra-operative diagnosis tools, able to detect individual cholesteatoma cells.

There are different techniques to diagnose cholestesatoma with the MRI, such as delay contrast-enhanced T1-weight and echo-planar diffusion-weighted. The latter technique showed more reliable results [22] [23] (Fig. 4). Vercruysse et al. [22] performed a study to assess an echo-planar diffusion-weighted MR imaging for detecting the primary acquired (55 patients) and the residual cholesteatoma (45 patients). In the first group, the diffusion-weight imaging (DWI) method detected 89% of cases with sensitivity and specificity values of 81% and 100%, respectively. In the second group, only one of seven surgically verified residual cases was correctly diagnosed using DWI, with sensitivity and specificity values of 12.5% and 100%, respectively.

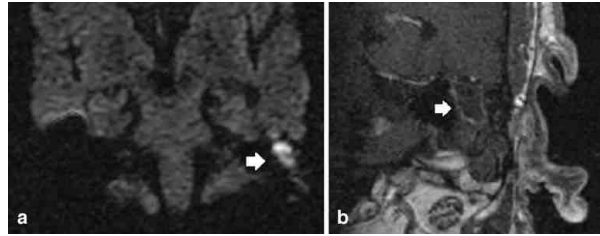


Fig. 4. The arrow represents primary acquired cholesteatoma [22], where (a) echo-planar DWI, (b) T1-weight.

Research on diagnostic imaging: The detection of the cholesteatoma cells throughout the intra-operative phase is a real problem. It is difficult for the surgeon to visualize the lateral regions hidden within the middle ear cavity. Moreover, oto-microscope is based on white-light imaging which is hampered by blood and does not allow for a clear distinction of small cholesteatoma masses. Therefore, one of the following methods could be used during the intervention in order to perform a real-time, reliable, cholesteatoma diagnostic.

First, ultrasound imaging [24] is widely used in intravascular, abdominal, gynaecologic and many other medical applications. To our knowledge, this method has not been applied for cholesteatoma screening but it was involved in other otological applications. Indeed, a high-frequency ultrasound system for imaging the auditory system was proposed in [25]. Ex-vivo experiments were done to obtain 3D images of ossicles and the tympanic membrane by using a  $6mm$  diameter probe. Also, 2D images of the cochlea were taken through the round window membrane. The system provides  $50\mu m$  axial resolution, and lateral resolution varying from  $80\mu m$  to  $130\mu m$  over a  $5.12mm$  scan

depth. The probe diameter was also miniaturized to  $1mm$  [26]. The system thus showed a better resolution than both the MRI and the CT but some water should be injected into the tympanic cavity for acoustic coupling sake.

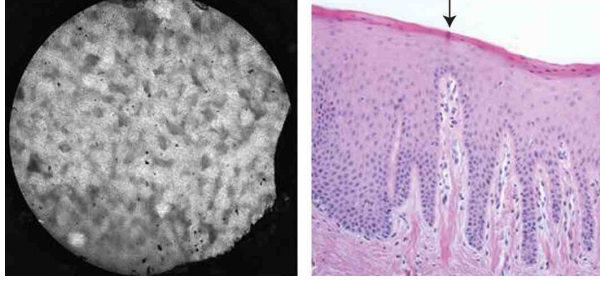


Fig. 5. Comparison of cholesteatoma imagery between fluorescence (left) and histological (right), where the arrow presents the cholesteatoma [27].

Second, fluorescence imaging [28] [29] is based on distinguishing the wavelength of the light emitted by different substances. It could be applied during the surgery to locate the remaining cholesteatoma cells. However, the surface of tympanic cavity must be stained with a contrast agent (e.g., proflavine) before taking images in order to discriminate normal and infected epithelial tissues. This technique was used in [27] [30] for realizing a fiberoptic endoscope that has a diameter of  $1mm$ . The ex-vivo experiments indicated that the mean accuracy, sensitivity and specificity were 95%, 98% and 92% respectively, and the resulting images are shown in Fig. 5. Moreover, the diameter of fiberoptics could vary from  $2.2mm$  to  $0.3mm$  as reported in [31], making them suitable for use in a minimally invasive middle ear surgery.

Third, OCT is a recent imaging technique [32] [33] that has many applications in ophthalmology, cardiac and otology imaging. It showed better resolution than ultrasound [34] [35] [36] and fluorescence technique [37] for soft tissues imaging.

Many designs of endoscopic OCT have been proposed, motivated by visualizing a sub-structure inside cavities and hollow organs [38] [39]. In fact, there are many works that deal with OCT for imaging various features in the middle ear, such as structures [40] [41] [42], motion of ossicles [43], chronic otitis media [44] [45], precancer and cancer mucosa [46].

Regarding cholesteatoma, a clinical study was conducted for imaging cholesteatoma using OCT and comparing the results with conventional observations obtained by binocular microscopy and histology [47]. In-vivo experiments were performed on 10 patients (5 males and 5 females) by inserting the OCT probe into the tympanic cavity under microscopic guidance, after surgical exposure. The

OCT images exhibit significant differences in signal intensity between normal tissues and those infected (Fig. 6) thanks to a claimed cross-section resolution around  $10\mu m$  and penetration depth around  $1mm$ . However, the probe had a  $2.7mm$  diameter which is somewhat large for examining certain areas (e.g., the posterior superior quadrant of the middle ear) because the probe may injure the stapes.

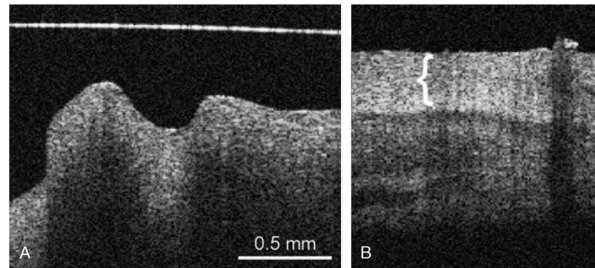


Fig. 6. OCT image of (A) normal mucosa; (B) cholesteatoma layer (bracket) over the mucosa [47].

#### E. Treatment

The main goal of the treatment is to create a dry and disease-free ear by fully eliminating the cholesteatoma and the chronic infection. So far, only a surgical procedure is regarded as offering the potentiality of excising all cholesteatoma cells. Depending on the infection site, various techniques are used to gain access to the middle ear cavity [48]: i) through the ear canal (transcanal approach), ii) through an incision in the auricle (endaural approach), or iii) through an incision in the mastoid bone behind the auricle (postauricular approach or mastoidectomy). The latter one is the most frequent for cholesteatoma surgery. It consists of creating a passage through the mastoid air-bony cells. There exist two kinds of mastoidectomy: canal wall up and canal wall down procedures. In the canal wall down (open) procedure, the posterior ear canal wall is removed as shown in figure 7(a). A large meatoplasty is created to allow adequate air circulation into the cavity in order that the sticky pieces of cholesteatoma could get out of the mastoid. In the canal wall up (closed) procedure, the ear canal wall is preserved as presented in figure 7(b). This procedure offers simpler post-operative care without regular cavity maintenance. It does not limit patients in their activities (e.g., hearing aids are easy to fit and there is a high tolerance for water exposure). Nevertheless, it may have more treatment failures (i.e., recurrent and/or residual cholesteatoma) than canal-wall down mastoidectomy, essentially due to the reduced access to the tympanic cavity and the manoeuvrability therein [49].

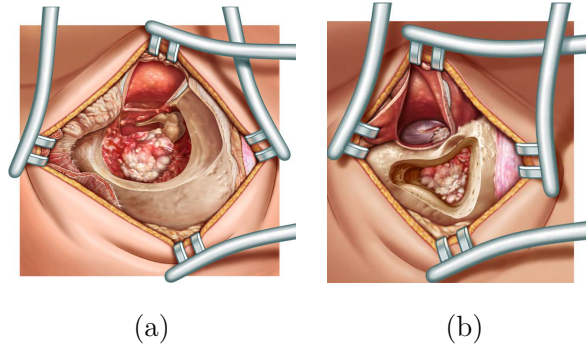


Fig. 7. Middle ear access by mastoidectomy: (a) canal wall-down and (b) canal wall-up procedures [48].

Most often, these procedures are performed under oto-microscopy. Nevertheless, the latter is characterized by a restricted FOV (Field Of View), and it does not allow visualising the lateral cavities, particularly with regard to the canal wall up approach. Therefore, there is a high possibility that cholesteatoma cells are left behind. If there is a doubt about the quality of resection, a second-look procedure is performed 6 to 18 months after the first surgery. Oto-endoscopy could be used beside oto-microscopy to offer a larger FOV during the intra-operative phase. In particular, oto-endoscope is expected to allow viewing the anatomic sites that are difficult to access under the oto-microscopy procedure [50] [51] [52] [53]. It also provides a minimally invasion surgical procedure during the second-look operation. Therefore, it could reduce the rate of residual cholesteatoma during the primary operation [54] [55] [56].

The corollary to surgery is the need for rehabilitation of ear function, the conservation or improvement of residual hearing, and the reconstruction of the tympanic membrane. Such complex task could be simplified or hopefully discarded by the use of a minimally invasive robot-assisted cholesteatoma surgery.

#### F. Ablation Tools

Cholesteatoma resection requires high expertise because it may appear under two different forms: i) a beaded appearance, or ii) a uniform layer above the middle ear mucosa [13]. For this reason, the surgeon should be equipped with adequate instruments (Fig. 8) and the latest technology of ablation tools, such as ultrasound and/or laser cutting tools.

For the moment, the use of HIFU (High-Intensity Focused Ultrasound) to destroy the aggregated cholesteatoma cells is not widely spread but it is used to target or to image diseased or damaged



Fig. 8. Kit of standard instruments used in an otologic surgery.

tissues in others parts of the human body, such as eye <sup>7</sup>, prostate <sup>8</sup> or breast. The ultrasound technology is not narrowed to remove soft tissue but it can also be used as ablation tool for hard tissue.

The piezosurgery device (Mectron Medical Technology <sup>9</sup>) is an ultrasound instrument ( $24.7-29.5kHz$ ) that is able to cut the bone while leaving the soft tissues untouched by the ablation process. This instrument is used in otologic surgery [57] to perform a mastoidectomy while preserving the facial nerve.

Furthermore, laser technology has wide application in otologic surgery to ablate hard and soft tissues. For instance, the BeamPath CO<sub>2</sub> laser system developed by OmniGuide Surgical <sup>10</sup> allows performing laser otosclerosis surgery [58] and cholesteatoma ablation.

Another study was conducted to evaluate the use of solid-state potassium titanyl phosphate (KTP) laser for diminishing the rate of residual cholesteatoma [59]. It showed that this rate was significantly reduced, where 1 out of 36 cases had residual cholesteatoma after laser surgery and 10 out of 33 cases without laser treatment.

Furthermore, a study was conducted to develop a laser treatment that selects the cholesteatoma cells based on the information obtained from a fluorescence imaging system [60]. In-vitro experiments had the objective to test the technical issues, as the photodynamic effect on cholesteatoma tissue and the different absorption enhancements. The system showed the ability to destroy up to 92% of cholesteatoma cells.

<sup>7</sup>Imasonic Medical Transducer [online]. <http://www.imasonic.com/Medical/Medical.php>

<sup>8</sup>Sonacare Medical [online]. <http://sonacaremedical.com>

<sup>9</sup>Mectron Medical Technology [online]. <http://medical.mectron.com/>

<sup>10</sup>omniGuide Surgical [online]. <http://www.omni-guide.com>

### III. Surgical robotic system

This section begins by proposing, without prior restriction regarding the available technology, the futuristic requirements for conducting an ideal robot-assisted cholesteatoma surgery. The aim of such a system is to execute a minimally invasive cholesteatoma surgery (see Section III-A). After that, the current technology is presented in Section III-B. This section reviews the previous robotic systems which are implemented for the otologic surgery. These systems represent an interesting basis of work for the future development of a robotic system dedicated to cholesteatoma surgery.

#### A. Ideal Requirements for Robot-assisted Cholesteatoma Surgery

This part shows the futuristic requirements and specifications needed for implementing an ideal system. Thereby, a novel surgical workflow is proposed here to satisfy the clinical demands. Besides that, the technical and scientific requirements are discussed for designing the different components of the desired system. Finally, the safety and the risk analysis are discussed within this part.

Middle ear micro-surgery needs a well-trained surgeon to overcome the clinical challenges which can be summarized as: i) the movements within the tiny space of the middle ear cavity while preserving the critical anatomical structures (e.g., ossicle chain, facial nerve and chorda tympani nerve), and ii) the limited FOV for inspection and the manipulation of rigid surgical instruments within the middle ear cavity. Thus, the ideal system must be ergonomic for the surgeon in order to reduce his/her strain, and hence to reduce the hand tremor and to increase the precision (e.g., [61]). In addition, the system must help for performing dexterous micro-movements, and providing a visual feedback and/or an automated control based on the pre- and intra-operative images.

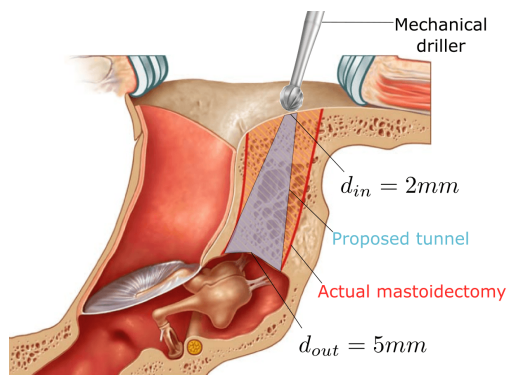


Fig. 9. A side view of the ear with the proposed minimally invasive tunnel.

### Clinical requirements

- New protocol: the new system creates a new workflow during the surgery
  - Pre-operative phase:
    - \* placement of fiducial markers
    - \* pre-operative imaging with CT and MRI devices
    - \* (semi)automatic segmentation of patient’s auditory system
    - \* (semi)automatic localization of cholesteatoma cells
    - \* construction a 3D surface/numerical model
    - \* plan the middle ear access tunnel (its diameter around 2-3mm) for drilling stage
    - \* plan the removal stage of cholesteatoma cells
    - \* produce a manual incision either in the external ear canal, in the auricle or behind the ear, or a combination of both
  - intra-operative phase:
    - \* automatic/manual registration of pre-operative plan to patient
    - \* bone ablation for creating the access tunnel (its depth around 25mm)
    - \* visualize the critical structure to the surgeon with the imaging tool (its outer diameter around 1 – 1.5mm) and determine the boundary of cholesteatoma region
    - \* automatic/cooperative cholesteatoma removal from the middle ear cavity and/or the ossicles with the ablation tool (its outer diameter < 2mm)
    - \* diagnostic in real-time the middle ear cavity for localizing residual cholesteatoma
    - \* execute the excision of residual cholesteatoma
- Risk analysis: sterilization, bio-compatible of end-effector material, infection risk, safety in surgeon/patient robot interface, risk during surgery and other specifications by laws (e.g., CE approval)

TABLE II

Summary of the clinical requirements and some important features.

New surgical workflow: The new intervention starts by fixing the fiducial markers to the patient skull during the pre-operative phase (see TABLE II). Such markers are beneficial for the segmentation and the registration processes since they will appear in the pre-operative images as reference points with respect to the target anatomy structures. CT images allow identifying the bony structures, while MR images are beneficial to locate the soft tissues as well as the cholesteatoma cells. The segmentation process collects the pre-operative slice images of CT and/or MRI in order

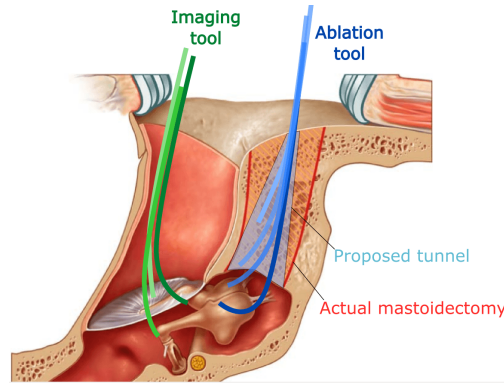


Fig. 10. A side view of the ear while manipulating different surgical tools.

to form a 3D surface model.

Then, the registration process [62] is performed at the beginning of the intra-operative phase for calibrating the image-guided robotic system. This process often consists of bringing the coordinate reference frames of the patient pre-operative images with the patient actual pose on the operation table. The calibration between the robot and the patient is very important and it will affect directly the system accuracy during the intra-operative phase. All these steps are performed with the help of a planning software throughout the pre-operative phase (e.g., [63]).

Based on the 3D model, the surgeon plans a safe access tunnel from the mastoid surface towards the middle ear cavity. The tunnel location should be optimized in order to drill the minimal distance for reaching the cholesteatoma cells. The tunnel dimensions should be less invasive, compared to the standard mastoidectomy procedure, while providing enough free space for manipulating the tools within the middle ear cavity. Therefore, a new minimally invasive tunnel is proposed to reach the middle ear cavity through the mastoid bone as depicted in Fig. 9. This new conical tunnel has a small diameter about  $2mm$  at its base which is located at the outer surface of the mastoid bone. This has the advantage for the patient to reduce risk of anatomical lesions and recovery time. Then the tunnel expands gradually until it reaches its maximum diameter at the upper region of the tympanic cavity.

During the intra-operative phase, a navigation software is responsible: i) to drill the planned tunnel in the temporal bone to reach the middle ear cavity, ii) to insert the surgical tool within the middle ear cavity for inspecting the suspected region while avoiding the other anatomical structures, and iii) to remove efficiently the cholesteatoma cells.

During ablation, a bimanual system is used (Fig. 10), as it is already done by the surgeon. The



first manipulator is used to drill the proposed tunnel. However, the way from the mastoid surface until the tympanic cavity could contain infected cells. Thereby, a novel mechatronics device is needed for an easy and fast exchange between the different tools (i.e., ablation and imaging tools). Such a device would be helpful for disinfecting the mastoid portion.

The second manipulator passes through the external ear canal and it is equipped with an OCT imaging probe to provide real-time 3D images (i.e., 3D optical biopsy) with micro-metric resolution. Such images are ideal to find out with high precision the location of cholesteatoma cells within the tympanic cavity. The OCT tool keeps the infected cells within its FOV and it guides automatically the ablation tool to scatter and suck out the infected cells.

## B. Otological surgical robotic systems

During the standard middle ear surgery, there are mainly two challenges that face the surgeon: i) limited FOV, and ii) tools rigidity. Therefore, the following classification provides inspiring examples to solve these challenges. Beside that they are useful to achieve the requirements in Section III-A.

The following classification arranges two groups of surgical robotic systems according to their medical applications. The first group is specifically dedicated to inner ear surgery, while the second group gathers the middle ear surgical robotic systems. For each system presented below, its strengths and weaknesses will be analyzed and the improvements towards cholesteatoma surgery will be suggested.

The majority of otological robotic systems are dedicated to cochlear implantation for treating a sensorineural hearing loss. This surgery is divided into two main steps: i) the first one is to create a passage to the inner ear, and ii) the second one is to insert the electrode into the cochlea (e.g., [64] [65]). Cochleostomy has the aim to reduce the required size of the mastoidectomy to a tunnel just larger than the inserted electrode (i.e.,  $1.5 \sim 2\text{mm}$ ) for reaching the inner ear. The created tunnel begins at the outer surface of the mastoid, passes through the facial recess and terminates in the middle ear in front of the round window. The required accuracy may be achieved by a robotic system, such as proposed in [66] [67].

Other robotic systems perform stapedectomy, which is the replacement of the stapes bone by an artificial prosthesis to treat a conductive hearing loss (e.g., [68] [61]). This surgery enters the middle ear through the external ear canal. As far as we know, there is not a robotic system that is dedicated to cholesteatoma surgery but the technology used in the following systems could be helpful to implement our objective system. The following part is divided into two classes: i) the

robotic systems that works in the inner ear to perform a cochleostomy, and ii) the other systems that works in the middle ear to perform a mastoidectomy or a stapedectomy.



Fig. 11. Da Vinci system in an operation room during cochlear implantation surgery [69].

**Strengths:** The master console provides a planning software and 3D environment reconstruction. This study extends its capacity by adding augmented reality for helping the surgeon. The tele-operated slave robot has a good accuracy for tool positioning.

**Weaknesses:** This system is very expensive and its size is very huge for executing small movements within the middle ear.

**Improvements:** Reduce size and costs. Add adequate tools for middle ear surgery.

1) Inner ear surgery: A cochlear implantation surgery was conducted with the Da Vinci<sup>11</sup> surgical system [69] (Fig. 11). This commercial system was originally dedicated to urologic surgery. It was adapted for performing mastoidectomy and image-guided electrode insertion. A custom tool adaptor is fabricated to hold a 8mm drilling tool and to shift its axis by 30° in order to be parallel with the endoscope axis. In fact, it is beneficial to use the different components of this commercial system, as its master console, its slave robot arm (which equipped by a driller, a 3D stereo-endoscope, and a suction/irrigation tool), a CT scanner, and a planning software. Cadaverous experimentations were done in two cases: i) the first case was done on a left temporal bone, and ii) the second one was done with augmented reality on right temporal bone. The operation was completed without any violation of critical structures and it took around 160 minutes per side.

For comparison, the current manual surgical intervention of cholesteatoma takes around 120 minutes by a senior surgeon, while it would take around 240 minutes by a junior surgeon. However, this system is too expensive and bulky. This is why dedicated robots were developed as shown below.

Another robotic system for cochlear implantation was proposed in [70] [72] [73]. The system uses an industrial robot (KUKA KR3) with 6-DOF to drill a tunnel through the facial recess (Fig. 12(a)).

<sup>11</sup>Intuitive Surgical, Inc. [online]. [http://www.intuitivesurgical.com/products/davinci\\_surgical\\_system/davinci\\_surgical\\_system\\_si/](http://www.intuitivesurgical.com/products/davinci_surgical_system/davinci_surgical_system_si/)



(a)



(b)

Fig. 12. (a) Robotic system for cochlear implantation [70]; (b) device for automated insertion of the electrode [71].

Strengths: the system consists of a planning software, an image-guided control, an optical navigation system, a milling tool and an insertion control of electrode

Weaknesses: Industrial robot is good for testing the control laws but it is not compatible with the clinical applications. The system is only equipped with a hard tissues ablation tool. The targeting error is too large.

Improvements: Reduce the robot size and increase its resolution. Develop a soft tissue ablation tool and a control software for guiding the ablation tool inside the patient body. Increase the accuracy of navigation system. Reduce the targeting error by half its current value.

It is also equipped with a flat-panel volume CT, a commercial planning software and an image-guided control software. The system uses three markers that consist of infrared light reflecting spheres to detect the pose of the tool tip via the stereo-optical navigation system, with an error less than  $0.35mm$ . The objective of the tracking system is to get rid of robot absolute positioning errors. Five fiducial markers are also attached on the patient for registration and motion tracking. The system was tested on ten human cadaveric temporal bones, where nine out of ten (90%) procedures were completed without complications. These tests indicated that the targeting mean deviation error was about  $0.5mm$ , essentially due to the calibration errors. In addition, a mechatronic device was designed [71] for automated insertion of the electrode array within the inner ear (Fig. 12(b)). Other systems similar to this one are proposed, for instance [74] [75].

The next robotic platform [76] will overcome the drawbacks of the previous system [73] by: i) implementing a robot structure suitable for clinical applications, and ii) reducing the optical tracking accuracy and the targeting error.

An experimental robotic system [76] [63] was also built at ARTORG center for a stereotactic cochlear electrode implantation. A mechanical driller performs a  $1.8 \sim 2mm$  tunnel from the surface

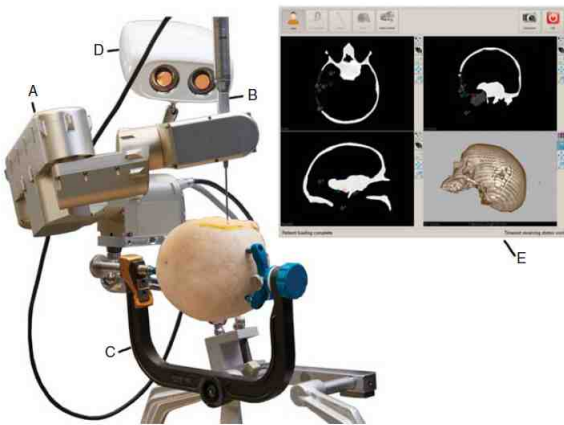


Fig. 13. Different components of ARTORG robotic system: (A) robot arm; (B) surgical driller; (C) head clamp; (D) optical tracking; (E) touch screen as the interface to the planning software [76].

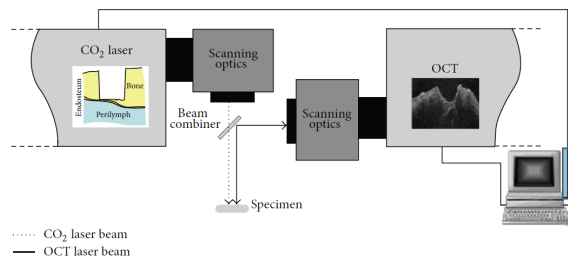
**Strengths:** The robotic system is suitable for realistic clinical applications, especially for creating a tunnel to the tympanic cavity. It also presents a good optical tracking accuracy and targeting error.

**Weaknesses:** The system is not prepared for performing the second phase of cholesteatoma surgery. It is missing soft tissues cutting tool, bendable end-effector, imaging tool for detecting cholesteatoma and control software for guiding the robot during the second phase.

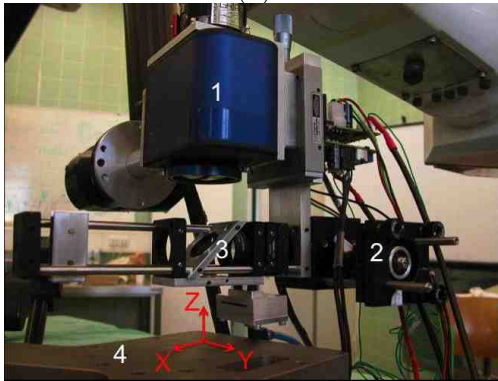
**Improvements:** bendable ablation tool for removing soft tissues and imaging tool should be added. A mechatronics device for exchanging between tools would be helpful.

of the mastoid to reach the round window. Figure 13 shows the different components of the system. The robot is a custom-built high resolution 5-DOF serial arm which is mounted on the operation table thanks to its light weight ( $5.5kg$ ). A high accuracy optical tracking system ( $< 0.05mm$ ) is used to register a pre-operative plan to the patient, and to control the tool position. A planning software enables a semi-automatic segmentation of the mastoid bone, the surrounding critical anatomical structures and the target ones. The planning software also automatically performs the fiducial registration with a sub-millimetric accuracy (around  $0.1mm$ ) and guides the definition of a safe trajectory. The patient's head is fixed with a non-invasive head clamp and an optically tracked dynamic reference base is attached to the patient to detect any small patient's movement. During the drilling stage, the system estimates the tool position continuously based on the relation between the force applied by the driller and the bone density [77]. Additional safety algorithms are employed to ensure a safe and effective drill path, such as monitoring the facial nerve to ensure its safety during this stage [78]. The robotic system was tested on eight human heads and the experiments showed a  $0.18mm$  mean accuracy [79].

Furthermore, a study was conducted [80] [82] to perform a 1-DOF laser cochleostomy guided by an OCT beam. The laser provides a clean cut on the bone with no significant thermal injury to the surrounding tissue. Compared to the conventional surgical burrs, laser allows a contactless removal of the bone tissue in the absence of any mechanical stress onto the fragile structures. It is also



(a)



(b)

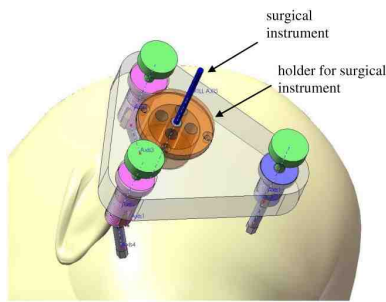
**Strengths:** Proof of concept to perform a laser bone removal guided by an OCT imaging system. The system accuracy is good. Notable patient tracking system by using OCT.

**Weaknesses:** The system setup has a big size and it is difficult to use in real clinical applications. For creating the tunnel to the tympanic cavity would take too long by using laser, but it is good for targeting small area with high accuracy.

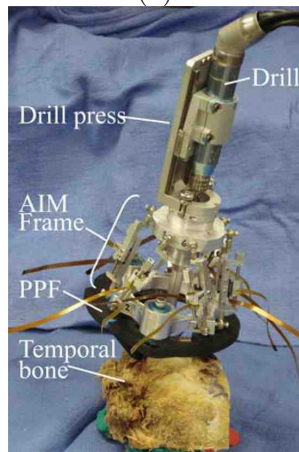
**Improvements:** The laser and OCT tools should be integrated into a bendable end-effector for increasing the system dexterity.

Fig. 14. (a) Schematic diagram of conceptual setup between the laser and the OCT [80]; (b) experimental setup; where (1) CO<sub>2</sub> laser, (2) OCT, (3) beam combiner, (4) 6-DOF parallel platform [82].

considered to be safer for the patient by generating much less bone-debris and reducing the risk of inflammatory tissue. In order to detect the remaining depth to be drilled, an OCT is located coaxially to the laser tool. Figure 14 shows the system setup that is done to overlap the working space of both systems (i.e., OCT and laser) with the help of beam combiner. This setup allows also the control of laser ablation and the OCT scanning simultaneously: the laser pulses is guided according to the thickness of the residual bone layer above the critical structure. During the whole procedure, the patient may have a small displacement which affects the procedure accuracy. As a consequence, a patient tracking system is important to localize the laser position with respect to the patient's position. For this reason, the OCT was used to track the round window by locating small laser-ablated landmarks surrounding the latter. During ex-vivo experimental evaluation on cadaver cochleas, the preliminary measurements in OCT scans indicated that the mean absolute



(a)



(b)

Strengths: The system provides good targeting error. The bone attached robot eliminates all the need to track patient's movements.

Weaknesses: The system segmentation error is quite high. Soft tissues ablation tool, diagnostic imaging tool and bendable end-effector are missing. It would be difficult to exchange between the different tools with the current configuration.

Improvements: Add adequate tools for middle ear surgery, as imaging, biopsy and soft tissue cutting tools. Modify the current design to easily exchange between the different tools.

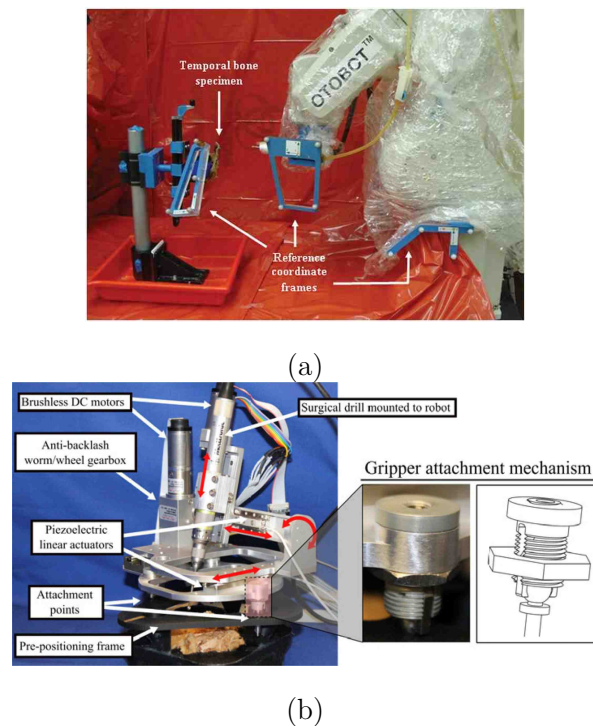
Fig. 15. Microtable: (a) early design concept [83]; (b) bone-attached parallel robot with preposition frame (PPF) and automatic image-guided microstereotactic (AIM) frame [84].

accuracy of tunnel shape was around  $20\mu m$ .

Another robotic system, called Microtable, was proposed in [83]. It is attached to the patient's head for executing cochleostomy. It has the advantage to eliminate the needs to track the patient's head. The Microtable is fabricated with a rapid prototyping technique and it is customized for each patient based on the drilled trajectory. The construction of the template takes six minutes. Afterwards the template is sterilized. The drilled trajectory is defined by a custom planning software (Fig. 15(a)) which collects the pre-operative CT images for automatic segmentation with an accuracy of approximately two voxels [87] (for an image resolution around  $0.3 \times 0.3 \times 0.4mm^3$ ) and the mean error to identify the temporal bone anatomy varies from  $0.5mm$  to  $0.3mm$  [88]. The software is also used to optimize the linear trajectory. Phantom experiments showed a mean drilling accuracy at

the target of  $0.37 \pm 0.18mm$ . The same concept was extended to perform automatic percutaneous cochlear implantations [84] with a parallel robot structure (Fig. 15(b)). It was also tested on a phantom model and cadaver temporal bones, where the targeting errors are  $0.2 \pm 0.07mm$  and  $0.38mm$ , respectively.

2) Middle ear surgery: The robotic systems in [85] [86] are proposed for executing mastoidectomy. These systems are equipped with a CT scanner and a planning software for segmentation of anatomical structures and registration procedure. On the one hand, the system in [85] called OTOBOT is composed of an industrial robot (Mitsubishi RV-3S) and a custom-built end-effector to hold the surgical driller. In addition, optical markers are placed on the end-effector and on the patient for measuring the instantaneous pose of the robot and that of the patient by using an optical tracking system (Fig. 16(a)). The tracking system claimed a  $0.25mm$  accuracy. The whole system was tested on three cadaveric temporal bones, where the percentage of each removed volume were



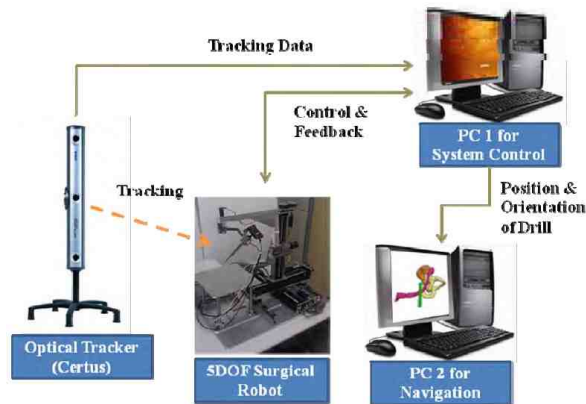
Strengths: The bone-attached robot [86] does not require an optical tracking system.

Weaknesses: Only the bone ablation tool is available in both systems. The components of [85] are not adapted to clinical applications and the tracking error is relatively large. The system [86] cannot manipulate tools within the middle ear through the external ear canal.

Improvements: Add soft tissue ablation tool for both systems. Reduce the size of optical marker of system [85] and the tracking error.

Fig. 16. (a) OTOBOT robotic system for mastoidectomy [85]; (b) bone attached robot with the positioning frame [86].

97.7%, 99.99% and 96.05%, respectively. On the other hand, the system in [86] used another strategy for proceeding to the operation. A custom-built 4-DOF serial robot attached to the temporal bone with a positioning frame to eliminate the need of an optical tracking system (Fig. 16(b)). The system showed a mean accuracy of  $0.5mm$  on a phantom milling test.



Strengths: Significant kinematic structure for RCM. Cooperative control for eliminating the hand tremor.

Weaknesses: The system does neither have soft tissues cutting tool nor cholesteatoma imaging tool.

Improvements: Add the required tools and a mechatronics device for exchanging between tools.

Planning software is necessary to carry out automatically the mastoidectomy.

Fig. 17. Configuration of robotic system mastoidectomy [89].

Another image-guided robotic system [89] was proposed to perform mastoidectomy. A serial robot is used and it has a special kinematic structure with 5-DOF (Fig. 17). This structure has the objective to impose physical constraints on the surgical tool in order to respect the anatomical constraints of the entry point (i.e., fulcrum point). The system is also composed of an optical tracker and a navigation software. Such a software activates a warning mode when the driller approaches the critical structures, such as the facial nerve. In practice, the safe margin was set to  $3mm$  which is relatively "large" with respect to the targeted application. In addition, the system provides the surgeon with human-robot collaboration control for compensating the hand tremor.

A tele-operated prototype robot was proposed for carrying out a stapedectomy surgery through the external ear canal. This assistant system is named RobOtol [91] [90] [92] and it is composed of a slave robotic arm and a master joystick (Fig. 18). The system was initially designed for using three arms simultaneously. Each arm has 6-DOF and its dimensions are optimized for the middle ear surgery. The system main objective is to enhance the FOV provided to the surgeon for performing more complex gestures. The surgeon moves the robotic arm via the joystick while looking to middle ear structures by using either conventional otomicroscopy or a  $4mm$  endoscope. During the operation, the stapes bone is removed and a drilled hole of  $0.5mm$  into the incus bone



is done, afterwards the prosthesis is fixed carefully between the incus bone and the round window of inner ear. The required force during the surgery varies between  $0.7N$  to  $3N$ .

Another tele-operated system for stapedectomy called Micromanipulator System (MMS-II) [93] allows the surgeon for manipulating the standard surgical instruments within the middle ear. The system is composed of a small manipulator with 4-DOF and a control console with two joysticks (Fig. 19(a)). Its feature extends to measure the distance between the stapes and the incus for deciding the required prosthesis length [94]. This is done by touching the two anatomical structures using the micro-instrument, then the system calculates and visualizes their relative distance. An alternative system, called Micro-Macro Telematulation System (MMTS) [95], was proposed to enhance the workspace and the features of the MMS-II system (Fig. 19(b)). The system is composed of a joystick console fixed on the operation table, a macro-manipulator arm (6-DOF with  $1.6mm$

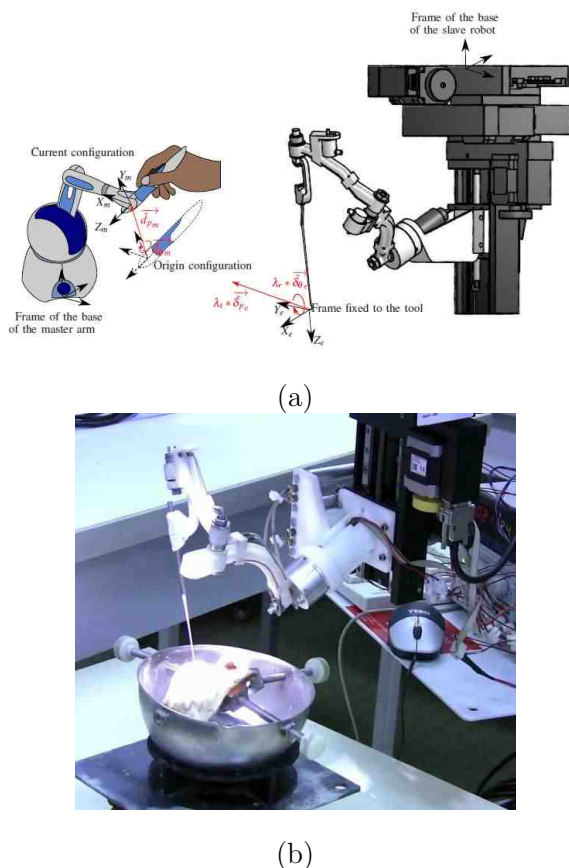


Fig. 18. (a) Master-slave RobOtol surgical system, (b) experimental setup of RobOtol [90].

**Strengths:** Good tools for middle ear surgery, as micro-scissor or laser, driller and endoscope. Specific kinematic structure that allows manipulating tools within the middle ear through the natural orifice of the external ear canal. Tele-operated robot allows eliminating the surgeon's hand tremor.

**Weaknesses:** The rigid tools are ideal to work in the middle region of tympanic cavity (atrium/meso-tympanic) but they cannot reach the upper or lower regions (attic/epitympanic recess or hypotympanic) where cholesteatoma develops.

**Improvements:** The end-effector has to gain some bending characteristics in order to reach the different regions of tympanic cavity and avoid critical anatomical structures. Adding the possibility to get into the middle ear through the temporal bone and a planning software is needed. Adequate tool for cholesteatoma ablation is also required, as well as the control software for navigation and automated guidance.

positioning accuracy) for large displacements, and robotic fingers that hold a tool adaptor. The latter part was designed for gripping different tools, such as the MMS-II micro-manipulator for fine movements, an endoscope or a driller. It is also equipped with four force sensors for measuring the applied force at the instrument tip.

Similar to MMS-II and MMTS, the Robotic Ear Nose and Throat Microsurgery System (REMS) [96] was also proposed for manipulating standard rigid tool during an otolaryngologic procedure. The previous systems are good for manipulating the standard surgical tools. However, these tools are characterized by their rigidity which represents a challenging problem for the surgeon since it is difficult to reach the lateral region within the middle ear cavity through small incision hole.

In order to circumvent this problem, the authors in [97] proposed a bendable endoscope to visualize the cholesteatoma within the middle ear cavity. The original system was implemented for eye surgery [98] [99]. The novel wrist consists of a nitinol tube with several asymmetric cutouts. The tube can bend with the actuation of a single tendon, as well as translate along one axis and rotate about its central axis. The outer diameter can be miniaturized below  $2mm$ . A phantom model of the middle ear cavity was fabricated by a 3D printer. The experimental work showed that the proposed bendable endoscope increased the visibility of sinus tympani region by 74.16%, compared with a straight endoscope.

The study of continuum robots (or bendable robotics) is a very vast and an active research topic [100] [101] [102], notably throughout the last two decades. Therefore, an adequate bendable tool for otologic surgery needs more investigation in this in the future.

#### IV. Guidelines for the required micro-robotic assisted cholesteatoma surgery

The previous sections presented the current state of otologic robotic systems, as well as the ideal requirements for micro-robotic assisted cholesteatoma surgery. As a complement, this section provides the guidelines for designing and implementing the required system based on the current technology for eliminating efficiently the cholesteatoma cells.

##### A. Clinical

The required robotic system should extend the surgeon dexterity in confined spaces, as well as it should be ergonomic for the surgeon. It should also offer an accurate diagnostic and reliable enough for performing a minimally invasive surgery. The treatment outcomes should be increased: i) by reducing the time, cost and hospitalization stay, and ii) by eliminating the second-look operation.

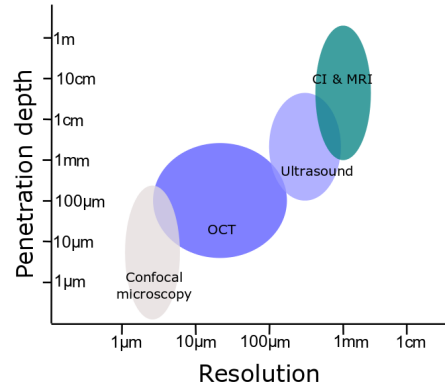


Fig. 20. Comparison between the different imaging techniques [103].

The first priority during the design process of a surgical robotic system is the patient's safety. As a result, analyzing the risk that may happen is a crucial step during the design phase.

The residual cholesteatoma cells are the main problem during the surgery. Thus, it is needed to remove completely these cells throughout the first surgery. The intra-operative imaging tools have an important role to detect the residual cells which are smaller than  $3mm$ . Fig. 20 shows that the CT and MRI cannot satisfy the latter criteria, while the fluorescence imaging (confocal microscope) has the best resolution compared to the others tools. A fibre-based fluorescence can also reach a small external diameter. However, it provides real-time 2D imaging with only a few micro-meters in depth. The ultrasound and OCT can provide a deeper view through the tissue. It is difficult with the current technology to obtain a small ultrasound probe (i.e., its diameter is smaller than  $1mm$ ), while the OCT can easily reach a small diameter. Therefore, an optimal solution would be to combine an OCT and fluorescence on the same fibre-optic in order to obtain a good resolution with enough depth.

After the detection of residual cholesteatoma cells, the laser is a good ablation tool for burning out these tiny cells. It also has the advantage to be integrated with a fibre-optic cable. Thereby, the same cable could be used either an imaging or ablation tools.

## B. Robotic Structure and Computer-Assisted Surgery

A surgical robotic system can generally be divided into two main parts: the robot structure and the software assisting the surgeon. The latter is often named CAS (Computer-Assisted Surgery) software and it is helpful to improve the ergonomics, the accuracy and the repeatability of a surgical robotic system. The development of both aspects is essential for the improvement of these systems.

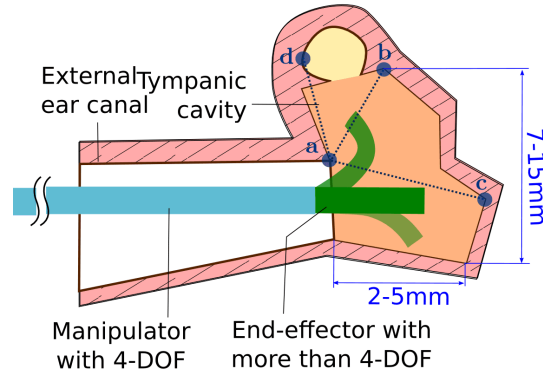


Fig. 21. Conceptual schema to demonstrate the required DOF for the manipulator and the end-effector.

There are many reviews [3] [104] [105] [106] [107] that present the historical development of surgical robotic systems and describe their components. However, our description is originally focused with the ear surgery in mind.

**Robotic structure:** The choice of the robot kinematic structure is an essential feature in order to achieve the design requirements (TABLE III). A typical medical robot structure is composed mainly of its manipulator and its end-effector.

The manipulator holds the end-effector and it offers a large (macro) displacement in order that the surgeon could easily change the surgical tool location with respect to the patient's head. It is also beneficial that the surgeon could use the oto-microscope while the robot is executing the desired task (e.g., RobOtol [90]). Beside that this special kinematic structure can perform the fulcrum effector (or remote centre of motion). The authors in [108] reviewed these structures which are mechanically constrained. However, these constrained motion can be achieved by a software controller, i.e., a computer-assisted surgery interface [109] in order to release some constraints from the mechanical design. Thereby, this controller can guide different robotic structures, such as ARTORG robot or RobOtol system, to execute the proposed tunnel in Fig. 9. Consequently, the manipulator's DOF should be equal or greater than 4-DOF to enter through a fulcrum point.

**DOFs of the end-effector:** For a certain number of cases (less than 50% where the exact number does not provided by the actual clinical database), the cholesteatoma cells are found in a convex region as presented by the light orange region in Fig. 21. During such situation, an end-effector with 3-DOF can reach all points within this convex region. However, there are some cases (more than 50%) where the development region of the cholesteatoma cells is non-convex. This non-convex region is formed by the unification of the light yellow region with the light orange one as depicted

in Fig. 21. Consequently, the end-effector should have more than 4-DOF to reach all cholesteatoma cells. Therefore, it is naturally to choose directly a end-effector with 4-DOF.

Computer-assisted surgery: The CAS software is mainly composed of proprioceptive and exteroceptive sensors, controllers and a surgeon-robot interface. The proprioceptive sensors (e.g., joint sensors) collect data about the internal state of the robot, while the exteroceptive sensors (e.g., CT [110], MRI [111], OCT [80] [42], ultrasound [112], camera(s) [113] and/or force sensor) provide information about the external environment.

A low-level controller is used to convert a control pose/velocity from the task-space into the joint-space. Beside that, a high-level controller would be helpful for performing more complex motion. For instance, a task priority controller allows following precisely a reference path while maintaining the RCM constraints [113]. Such a controller is beneficial for medical applications, especially during the intra-operation of middle ear surgery. Despite that, the controller in [113] needs to be extended in order to guide an ablation process while using a 3D imaging source (e.g., OCT or ultrasound) and a bendable tool. By adding this feature, the intra-operative control software in the design requirements (TABLE IV) is ready to be integrated with the other parts.

The surgeon-robot interface is valuable for the communication interface which helps the surgeon to control the robot easily. All the previous components contribute to guide and track the robot structure either in a semi-automated (cooperative) mode or in a fully automated mode. For both modes, a planning software should be the first step before the intra-operative phase to accomplish three functions: i) identifying the different anatomical structures from the MRI and/or CT pre-operative images for creating a 3D surface model (Fig.22(a)), ii) optimizing the drilling trajectory from the temporal bone surface to the tympanic cavity while avoiding the damage of critical structures (curve planning), and iii) calibrating the robot initial position and orientation with respect to the patient's body (registration). On one side, the fully automated mode performs a pre-programmed motion defined by the surgeon. On the other side, the semi-automated mode cooperates with the surgeon in order to improve the surgery efficiency and it provides the surgeon with a continuous control.

<sup>12</sup>CamBar B1, Axios 3D GmbH, Germany. [online] <http://www.axios3d.de/EN/medical/products/trackingsys/cambarb1.html>

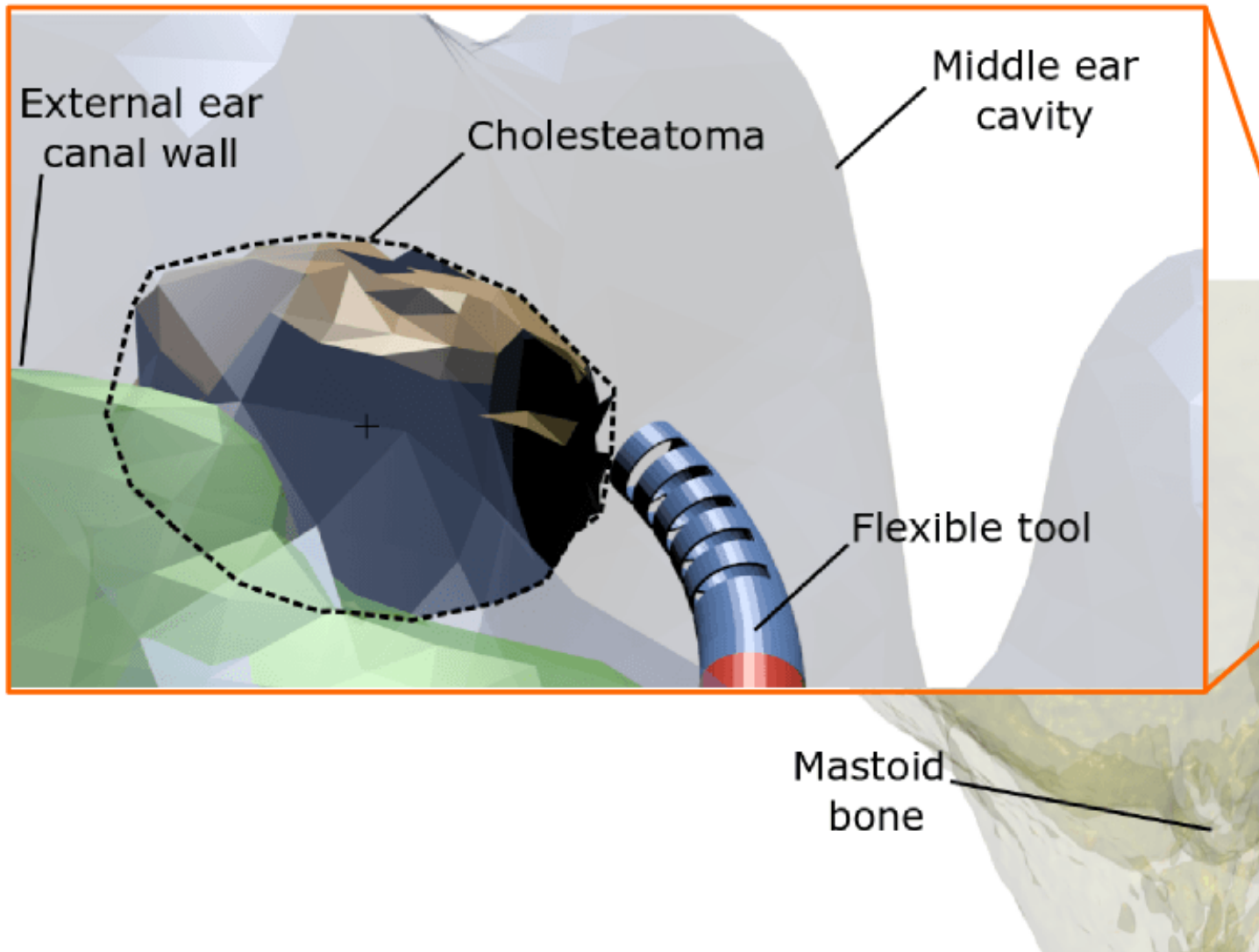
### C. Safety and risk analysis

Safety occupies an important aspect for designing and working with a surgical robotic system [3] [114] [115]. Indeed, there is not a method that guarantees safety with zero risk. Consequently, a comprehensive study is required to define the potential hazard that could be produced by the robot on the patient and the surgical staff, as [116] [117]. Hardware and software protections are also needed for avoiding undesired system failure or sudden robot movements, and pulling out the robot easily in such situations. In addition, the robotic system should be bendable and dexterous for avoiding the critical structures within the middle ear cavity. Another important features in safety are biocompatibility and sterilization of robot parts that are in contact with the patient's body. Lastly, the imaging system has an important impact on safety. The image quality contributes to construct an accurate 3D surface model of patient's anatomy, to detect the disease location and to guide the robot. The use of images globally increases the performances, including safety, but any error in the image exploitation may create a risk to the patient. Therefore, a specific risk analysis must be performed on that topic.

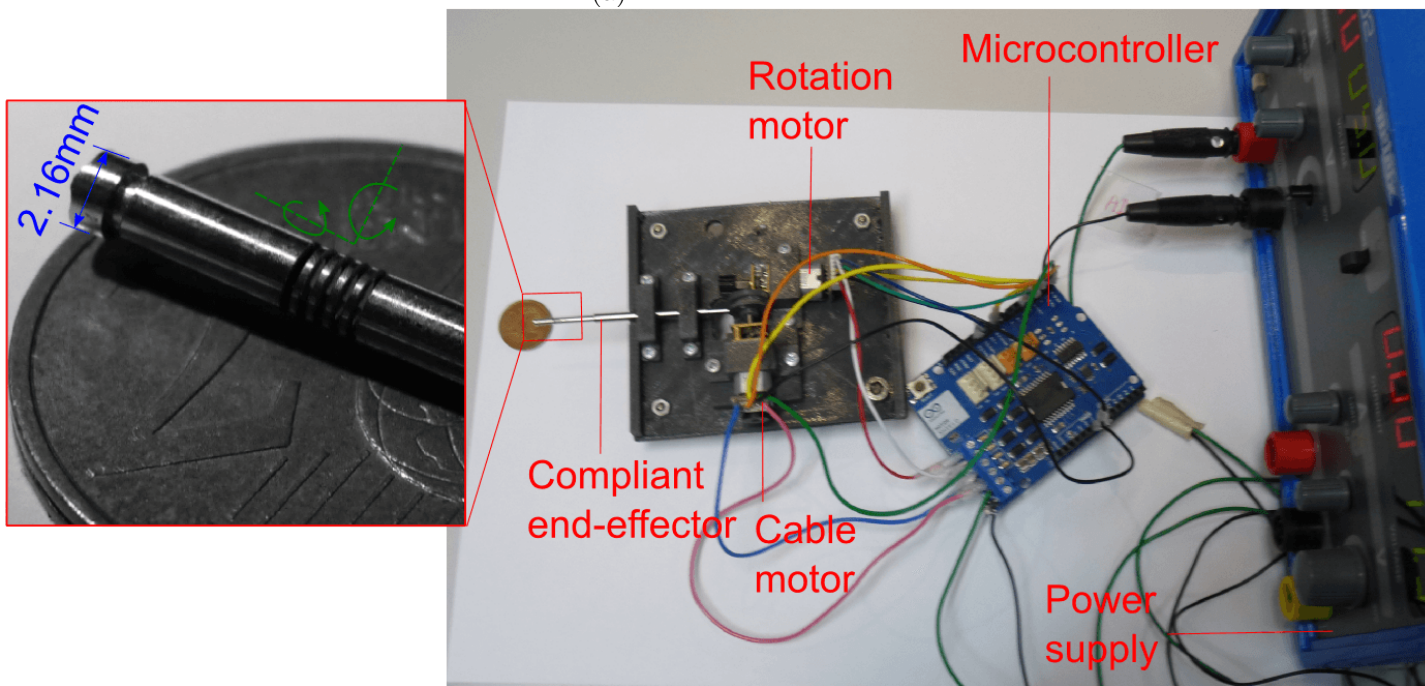
### D. Targeted Robotic Concept for Middle Ear Surgery

A first prototype was fabricated based on the model proposed in [97]. This reproduction from the literature allows a better understanding of the mathematical model. The prototype is composed of a bendable tube of Nitinol, as shown in Fig.22(b). This tube has rectangular cutouts in order to make the tube deflect easily from one side. This deflection motion is actuated by a cable. When the cable force is realised, the tube returns to its initial form. Additional rotation about the tube axis is possible.

Such a first prototype is relatively simple for fabrication compared to other actuation types, for instance SMA (Shape Memory Alloy) [118] [119] and EAP (Electro-Active Polymers) [120] [121]. However, the measured deflection angle during the experiments was small (around  $42^\circ$ ) compared to the required one (around  $270^\circ$ ). Thereby, a new concept was proposed as depicted in Fig. 22(c). This concept makes a two stages micro-tool. The first stage is a cable-driven bendable tube which has new triangular cutouts in order to increase the deflection angle. The second stage could be actuated either by an EAP or a magnetic field. However, the integration of additional actuation sources with the micro-tool is challenging and it requires more detailed study.



(a)



(b)

## V. Conclusion

As far as we known, there is no robotic system that is capable to perform the cholesteatoma surgery. Therefore, this review showed the interdisciplinary research topics which aim for implementing an efficient and reliable assisted micro-robotic system dedicated to cholesteatoma surgery.

On the clinical side, the review begun by a detailed information about the cholesteatoma disease, its diagnostics, as well as its treatment which is a surgical procedure. Based on this analysis, it is required to investigate in the diagnostics imaging technique which is applicable during the intra-operative phase. Such an imaging technique is very helpful to detect the residual cholesteatoma cells. Besides that, it is required to study in details the safety of the new clinical protocol on the patient and the surgical staff. It is also needed to go further for the estimation of the required accuracy, velocity and forces.

On the engineering side, the miniaturization issue is a large scientific and technical challenge, especially in a tiny workspace as the middle ear cavity. As a result, the review showed the different robotic system dedicated to the inner ear and the middle ear cavity. These systems are summarized in TABLE VI. Briefly, the new robotic system should be ergonomic and overcome the rigidity problem by designing bendable micro-tools. Such quickly exchangeable bendable tools provide various functions in order to alternate between the ablation task (i.e., the hard tissues during the tunnel drilling and the soft tissues during the cholesteatoma excision) and the imaging task (i.e., scan the surrounding environment, search for the cholesteatoma cells and guide the excision process). A good and safe control strategy of the tool tip with a high accuracy and dexterity are also needed for increasing the visibility within the middle ear cavity. Finally, a clinical study should be done to prove the system performances.

## References

- [1] E. Olszewska, M. Wagner, M. Bernal-Sprekelsen, J. Ebmeyer, S. Dazert, H. Hildmann, and H. Sudhoff, "Etiopathogenesis of cholesteatoma," *European Archives of Oto-Rhino-Laryngology and Head & Neck*, vol. 261, no. 1, pp. 6–24, 2004.
- [2] B. D. Djurhuus, A. Skytthe, K. Christensen, and C. E. Faber, "Cholesteatoma in danish children—a national study of changes in the incidence rate over 34 years," *International journal of pediatric otorhinolaryngology*, vol. 79, no. 2, pp. 127–130, 2015.
- [3] R. D. Howe and Y. Matsuoka, "Robotics for surgery," *Annual Review of Biomedical Engineering*, vol. 1, no. 1, pp. 211–240, 1999.
- [4] B. J. Nelson, I. K. Kaliakatsos, and J. J. Abbott, "Microrobots for minimally invasive medicine," *Annual review of biomedical engineering*, vol. 12, pp. 55–85, 2010.



- [5] L. Dong and B. J. Nelson, "Tutorial-robotics in the small part ii: nanorobotics," *IEEE Robotics & Automation Magazine*, vol. 14, no. 3, pp. 111–121, 2007.
- [6] R. Renevier, B. Tamadazte, K. Rabenorosoa, L. Tavernier and N. Andreff, "Endoscopic Laser Surgery: Design, Modeling, and Control," in *IEEE/ASME Transactions on Mechatronics*, vol. 22, no. 1, pp. 99-106, Feb. 2017.
- [7] B. Tamadazte, A. Agustinos, P. Cinquin, G. Fiard, and S. Voros, "Multi-view vision system for laparoscopy surgery," in *International Journal of Computer Assisted Radiology and Surgery*, vol. 10(2), pp 195–203, 2015.
- [8] H. Gray, *Anatomy of the human body*. Lea & Febiger, 1918.
- [9] F. Legent, L. Perlemuter, and C. Vandenbrouck, *Cahiers d'anatomie ORL*. Masson, 1968.
- [10] C. Abdala and D. H. Keefe, "Morphological and functional ear development," in *Human Auditory Development*. Springer, 2012, pp. 19–59.
- [11] C. Alper, *Advanced therapy in otitis media*. PMPH-USA, 2004.
- [12] J. McJunkin and R. Chole, "Clinical utility of mri for cholesteatoma recurrence," *Current Surgery Reports*, vol. 2, no. 8, pp. 1–7, 2014.
- [13] P. Bordure, S. Bailleul, O. Malard, and R. Wagner, "Otite chronique cholestéatomateuse. aspects cliniques et thérapeutiques." pp. 1–16, 2009.
- [14] H. Kemppainen, H. Puhakka, P. Laippala, M. Sipilä, M. Manninen, and P. Karma, "Epidemiology and aetiology of middle ear cholesteatoma," *Acta oto-laryngologica*, vol. 119, no. 5, pp. 568–572, 1999.
- [15] B. D. Djurhuus, C. E. Faber, and A. Skyttthe, "Decreasing incidence rate for surgically treated middle ear cholesteatoma in denmark 1977–2007," *Danish Medical Bulletin*, vol. 57, no. 10, p. A4186, 2010.
- [16] T. Fiedler, D. Boeger, J. Buentzel, D. Esser, K. Hoffmann, P. Jecker, A. Mueller, G. Radtke, D. Häfke, T. Bitter et al., "Middle ear surgery in thuringia, germany: a population-based regional study on epidemiology and outcome," *Otology & Neurotology*, vol. 34, no. 5, pp. 890–897, 2013.
- [17] J. L. Sheehy, D. E. Brackmann, and M. D. Graham, "Cholesteatoma surgery: Residual and recurrent disease a review of 1,024 cases," *Annals of Otology, Rhinology & Laryngology*, vol. 86, no. 4, pp. 451–462, 1977.
- [18] J. E. A. P. d. Aquino, N. A. Cruz Filho, and J. N. P. d. Aquino, "Epidemiology of middle ear and mastoid cholesteatomas: study of 1146 cases," *Brazilian journal of otorhinolaryngology*, vol. 77, no. 3, pp. 341–347, 2011.
- [19] B. De Foer, S. Nicolay, J.-P. Vercruysee, E. Offeciers, J. W. Casselman, and M. Pouillon, "Imaging of cholesteatoma," in *Temporal Bone Imaging*. Springer, 2015, pp. 69–87.
- [20] M. Ourak, B. Tamadazte and N. Andreff, "Partitioned camera-OCT based 6 DOF visual servoing for automatic repetitive optical biopsies," *IEEE/RSJ International Conference on Intelligent Robots and Systems (IROS)*, Daejeon, 2016, pp. 2337-2342.
- [21] S. Kösling and F. Bootz, "Ct and mr imaging after middle ear surgery," *European journal of radiology*, vol. 40, no. 2, pp. 113–118, 2001.
- [22] J.-P. Vercruysee, B. De Foer, M. Pouillon, T. Somers, J. Casselman, and E. Offeciers, "The value of diffusion-weighted mr imaging in the diagnosis of primary acquired and residual cholesteatoma: a surgical verified study of 100 patients," *European radiology*, vol. 16, no. 7, pp. 1461–1467, 2006.
- [23] H. Frickmann and A. E. Zautner, "Cholesteatoma– a potential consequence of chronic middle ear inflammation," *Otolaryngology*, vol. 5, no. 1, 2012.
- [24] G. t. Haar and C. Coussios, "High intensity focused ultrasound: physical principles and devices," *International Journal of Hyperthermia*, vol. 23, no. 2, pp. 89–104, 2007.

- [25] J. A. Brown, Z. Torbatian, R. B. Adamson, R. Van Wijhe, R. J. Pennings, G. R. Lockwood, and M. L. Bance, "High-frequency ex vivo ultrasound imaging of the auditory system," *Ultrasound in medicine & biology*, vol. 35, no. 11, pp. 1899–1907, 2009.
- [26] Z. Torbatian, R. Adamson, R. van Wijhe, R. Pennings, M. Bance, and J. Brown, "Imaging the auditory system: A new application of high-frequency ultrasound," in *IEEE International Ultrasonics Symposium (IUS)*, 2009, pp. 236–239.
- [27] L. L. Levy, N. Jiang, E. Smouha, R. Richards-Kortum, and A. G. Sikora, "Optical imaging with a high-resolution microendoscope to identify cholesteatoma of the middle ear," *The Laryngoscope*, vol. 123, no. 4, pp. 1016–1020, 2013.
- [28] T. J. Muldoon, M. C. Pierce, D. L. Nida, M. D. Williams, A. Gillenwater, and R. Richards-Kortum, "Subcellular-resolution molecular imaging within living tissue by fiber microendoscopy," *Optics express*, vol. 15, no. 25, pp. 16 413–16 423, 2007.
- [29] R. K. Orosco, R. Y. Tsien, and Q. T. Nguyen, "Fluorescence imaging in surgery," *IEEE reviews in biomedical engineering*, vol. 6, pp. 178–187, 2013.
- [30] J. A. Bradley, N. Jiang, L. L. Levy, R. Richards-Kortum, A. Sikora, and E. E. Smouha, "High-resolution microendoscope images of middle ear cholesteatoma and surrounding tissue: Evaluation of interobserver concordance," *Otolaryngology–Head and Neck Surgery*, vol. 149, no. 2 suppl, p. P100, 2013.
- [31] T. Karhuketo, P. Dastidar, E. Laasonen, M. Sipilä, and H. Puhakka, "Visualization of the middle ear with high resolution computed tomography and superfine fiberoptic videomicroendoscopy," *European archives of oto-rhino-laryngology*, vol. 255, no. 6, pp. 277–280, 1988.
- [32] A. F. Fercher, "Optical coherence tomography," *Journal of Biomedical Optics*, vol. 1, no. 2, pp. 157–173, 1996.
- [33] A. F. Fercher, W. Drexler, C. K. Hitzenberger, and T. Lasser, "Optical coherence tomography-principles and applications," *Reports on progress in physics*, vol. 66, no. 2, p. 239, 2003.
- [34] M. E. Brezinski, G. J. Tearney, N. Weissman, S. Boppart, B. Bouma, M. Hee, A. Weyman, E. Swanson, J. Southern, and J. Fujimoto, "Assessing atherosclerotic plaque morphology: comparison of optical coherence tomography and high frequency intravascular ultrasound," *Heart*, vol. 77, no. 5, pp. 397–403, 1997.
- [35] P. Patwari, N. J. Weissman, S. A. Boppart, C. Jesser, D. Stamper, J. G. Fujimoto, and M. E. Brezinski, "Assessment of coronary plaque with optical coherence tomography and high-frequency ultrasound," *The American journal of cardiology*, vol. 85, no. 5, pp. 641–644, 2000.
- [36] I.-K. Jang, B. E. Bouma, D.-H. Kang, S.-J. Park, S.-W. Park, K.-B. Seung, K.-B. Choi, M. Shishkov, K. Schlendorf, E. Pomerantsev et al., "Visualization of coronary atherosclerotic plaques in patients using optical coherence tomography: comparison with intravascular ultrasound," *Journal of the American College of Cardiology*, vol. 39, no. 4, pp. 604–609, 2002.
- [37] J. Lademann, N. Otberg, H. Richter, L. Meyer, H. Audring, A. Teichmann, S. Thomas, A. Knüttel, and W. Sterry, "Application of optical non-invasive methods in skin physiology: a comparison of laser scanning microscopy and optical coherent tomography with histological analysis," *Skin Research and Technology*, vol. 13, no. 2, pp. 119–132, 2007.
- [38] P. H. Tran, D. S. Mukai, M. Brenner, and Z. Chen, "In vivo endoscopic optical coherence tomography by use of a rotational microelectromechanical system probe," *Optics letters*, vol. 29, no. 11, pp. 1236–1238, 2004.
- [39] A. Burkhardt, J. Walther, P. Cimalla, M. Mehner, and E. Koch, "Endoscopic optical coherence tomography device for forward imaging with broad field of view," *Journal of biomedical optics*, vol. 17, no. 7, pp. 071 302–

- 071 302, 2012.
- [40] C. Pitris, K. T. Saunders, J. G. Fujimoto, and M. E. Brezinski, “High-resolution imaging of the middle ear with optical coherence tomography: a feasibility study,” *Archives of Otolaryngology–Head & Neck Surgery*, vol. 127, no. 6, pp. 637–642, 2011.
- [41] R. Heermann, C. Hauger, P. Issing, and T. Lenarz, “Application of optical coherence tomography (oct) in middle ear surgery,” *Laryngo-rhino-otologie*, vol. 81, no. 6, pp. 400–405, 2002.
- [42] S. S. Gurbani, P. Wilkening, M. Zhao, B. Gonenc, G. W. Cheon, I. I. Iordachita, W. Chien, R. H. Taylor, J. K. Niparko, and J. U. Kang, “Robot-assisted three-dimensional registration for cochlear implant surgery using a common-path swept-source optical coherence tomography probe,” *Journal of biomedical optics*, vol. 19, no. 5, pp. 057004–057004, 2014.
- [43] H. M. Subhash, A. Nguyen-Huynh, R. K. Wang, S. L. Jacques, N. Choudhury, and A. L. Nuttall, “Feasibility of spectral-domain phase-sensitive optical coherence tomography for middle ear vibrometry,” *Journal of biomedical optics*, vol. 17, no. 6, pp. 0605051–0605053, 2012.
- [44] C. T. Nguyen, W. Jung, J. Kim, E. J. Chaney, M. Novak, C. N. Stewart, and S. A. Boppart, “Noninvasive in vivo optical detection of biofilm in the human middle ear,” *Proceedings of the National Academy of Sciences*, vol. 109, no. 24, pp. 9529–9534, 2012.
- [45] H. R. Djalilian, J. Ridgway, M. Tam, A. Sepehr, Z. Chen, and B. J. Wong, “Imaging the human tympanic membrane using optical coherence tomography in vivo,” *Otology & neurotology: official publication of the American Otological Society, American Neurotology Society [and] European Academy of Otology and Neurotology*, vol. 29, no. 8, pp. 1091–1094, 2008.
- [46] A. Sergeev, V. Gelikonov, G. Gelikonov, F. Feldchtein, R. Kuranov, N. Gladkova, N. Shakhova, L. Snopova, A. Shakhov, I. Kuznetzova et al., “In vivo endoscopic oct imaging of precancer and cancer states of human mucosa,” *Optics express*, vol. 1, no. 13, pp. 432–440, 1997.
- [47] H. R. Djalilian, M. Rubinstein, E. C. Wu, K. Naemi, S. Zardouz, K. Karimi, and B. J. Wong, “Optical coherence tomography of cholesteatoma,” *Otology & neurotology: official publication of the American Otological Society, American Neurotology Society [and] European Academy of Otology and Neurotology*, vol. 31, no. 6, pp. 932–935, 2010.
- [48] H. Hildmann and H. Sudhoff, *Middle ear surgery*. Springer Science & Business Media, 2006.
- [49] J. Tomlin, D. Chang, B. McCutcheon, and J. Harris, “Surgical technique and recurrence in cholesteatoma: a meta-analysis,” *Audiology & neuro-otology*, vol. 18, no. 3, pp. 135–142, 2012.
- [50] P. Bordure, A. Robier, and O. Malard, *Chirurgie otologique et otoneurologique*. Elsevier Masson, 2005.
- [51] S. Ayache, B. Tramier, and V. Strunski, “Otoendoscopy in cholesteatoma surgery of the middle ear: what benefits can be expected?” *Otology & Neurotology*, vol. 29, no. 8, pp. 1085–1090, 2008.
- [52] D. Marchioni, G. Molteni, and L. Presutti, “Endoscopic anatomy of the middle ear,” *Indian Journal of Otolaryngology and Head & Neck Surgery*, vol. 63, no. 2, pp. 101–113, 2011.
- [53] B. Hanna, I. Kivekäs, Y.-H. Wu, L. J. Guo, H. Lin, J. Guidi, and D. Poe, “Minimally invasive functional approach for cholesteatoma surgery,” *The Laryngoscope*, vol. 124, no. 10, pp. 2386–2392, 2014.
- [54] J. M. Thomassin, D. Korchia, and J. M. D. Doris, “Endoscopic-guided otosurgery in the prevention of residual cholesteatomas,” *The Laryngoscope*, vol. 103, no. 8, pp. 939–943, 1993.
- [55] M. Badr-el Dine, “Value of ear endoscopy in cholesteatoma surgery,” *Otology & neurotology*, vol. 23, no. 5, pp. 631–635, 2002.

- [56] H. Sajjadi, “Endoscopic middle ear and mastoid surgery for cholesteatoma,” *Iranian journal of otorhinolaryngology*, vol. 25, no. 71, pp. 63–70, 2013.
- [57] A. Salami, M. Dellepiane, E. Proto, and R. Mora, “Piezosurgery in otologic surgery: four years of experience,” *Otolaryngology-Head and Neck Surgery*, vol. 140, no. 3, pp. 412–418, 2009.
- [58] S. G. Lesinski and K. Giesken, “Optical fiber for co2 laser otosclerosis surgery,” *Otolaryngology-Head and Neck Surgery*, vol. 139, no. 2 suppl, pp. P57–P57, 2008.
- [59] J. W. Hamilton, “Efficacy of the ktp laser in the treatment of middle ear cholesteatoma,” *Otology & Neurotology*, vol. 26, no. 2, pp. 135–139, 2005.
- [60] P. P. Caffier, U. Marzahn, A. Franke, H. Sudhoff, S. Jovanovic, A. Haisch, and B. Sedlmaier, “Laser-assisted cholesteatoma surgery: technical aspects, in vitro implementation and challenge of selective cell destruction,” *European Archives of Oto-Rhino-Laryngology*, vol. 265, no. 10, pp. 1179–1188, 2008.
- [61] D. L. Rothbaum, J. Roy, D. Stoianovici, P. Berkelman, G. D. Hager, R. H. Taylor, L. L. Whitcomb, H. W. Francis, and J. K. Niparko, “Robot-assisted stapedotomy: micropick fenestration of the stapes footplate,” *Otolaryngology-Head and Neck Surgery*, vol. 127, no. 5, pp. 417–426, 2002.
- [62] K. Cleary and T. M. Peters, “Image-guided interventions: technology review and clinical applications,” *Annual review of biomedical engineering*, vol. 12, pp. 119–142, 2010.
- [63] N. Gerber, B. Bell, K. Gavaghan, C. Weisstanner, M. Caversaccio, and S. Weber, “Surgical planning tool for robotically assisted hearing aid implantation,” *International journal of computer assisted radiology and surgery*, vol. 9, no. 1, pp. 11–20, 2014.
- [64] J. R. Clark, L. Leon, F. M. Warren, and J. J. Abbott, “Magnetic guidance of cochlear implants: proof-of-concept and initial feasibility study,” *Journal of Medical Devices*, vol. 6, no. 3, 2012.
- [65] J. Pile and N. Simaan, “Modeling, design, and evaluation of a parallel robot for cochlear implant surgery,” *IEEE/ASME Transactions on Mechatronics*, vol. 19, no. 6, pp. 1746–1755, 2014.
- [66] P. Brett, R. Taylor, D. Proops, C. Coulson, A. Reid, and M. Griffiths, “A surgical robot for cochleostomy,” in *29th Annual International Conference of the IEEE Engineering in Medicine and Biology Society (EMBS)*, 2007, pp. 1229–1232.
- [67] T. Klenzner, C. C. Ngan, F. B. Knapp, H. Knoop, J. Kromeier, A. Aschendorff, E. Papastathopoulos, J. Raczowsky, H. Wörn, and J. Schipper, “New strategies for high precision surgery of the temporal bone using a robotic approach for cochlear implantation,” *European archives of oto-rhino-laryngology*, vol. 266, no. 7, pp. 955–960, 2009.
- [68] P. Brett, D. Baker, L. Reyes, and J. Blanshard, “An automatic technique for micro-drilling a stapedotomy in the flexible stapes footplate,” *Proceedings of the Institution of Mechanical Engineers, Part H: Journal of Engineering in Medicine*, vol. 209, no. 4, pp. 255–262, 1995.
- [69] W. P. Liu, M. Azizian, J. Sorger, R. H. Taylor, B. K. Reilly, K. Cleary, and D. Preciado, “Cadaveric feasibility study of da vinci si-assisted cochlear implant with augmented visual navigation for otologic surgery,” *JAMA Otolaryngology-Head & Neck Surgery*, vol. 140, no. 3, pp. 208–214, 2014.
- [70] M. Leinung, S. Baron, H. Eilers, B. Heimann, S. Bartling, R. Heermann, T. Lenarz, O. Majdani, and G. CURAC, “Robotic-guided minimally-invasive cochleostomy: first results,” *GMS CURAC*, vol. 2, 2007.
- [71] A. Hussong, T. Rau, H. Eilers, S. Baron, B. Heimann, M. Leinung, T. Lenarz, and O. Majdani, “Conception and design of an automated insertion tool for cochlear implants,” in *30th Annual International Conference of the IEEE Engineering in Medicine and Biology Society*, 2008, pp. 5593–5596.

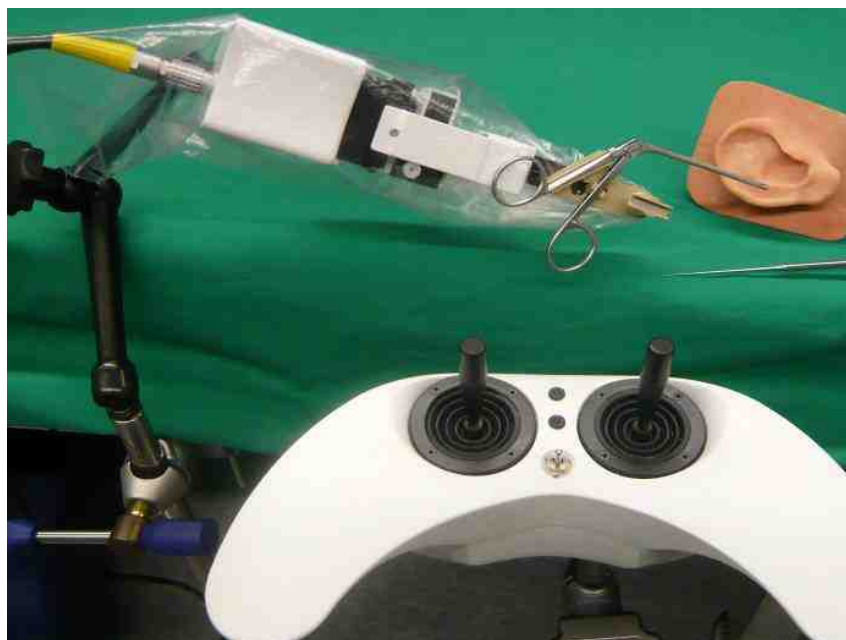
- [72] O. Majdani, T. S. Rau, S. Baron, H. Eilers, C. Baier, B. Heimann, T. Ortmaier, S. Bartling, T. Lenarz, and M. Leinung, "A robot-guided minimally invasive approach for cochlear implant surgery: preliminary results of a temporal bone study," *International journal of computer assisted radiology and surgery*, vol. 4, no. 5, pp. 475–486, 2009.
- [73] S. Baron, H. Eilers, B. Munske, J. Toennies, R. Balachandran, R. Labadie, T. Ortmaier, and R. Webster III, "Percutaneous inner-ear access via an image-guided industrial robot system," *Proceedings of the Institution of Mechanical Engineers, Part H: Journal of Engineering in Medicine*, vol. 224, no. 5, pp. 633–649, 2010.
- [74] J. Zhang, K. Xu, N. Simaan, and S. Manolidis, "A pilot study of robot-assisted cochlear implant surgery using steerable electrode arrays," in *Medical Image Computing and Computer-Assisted Intervention (MICCAI)*. Springer, 2006, pp. 33–40.
- [75] J. Zhang, W. Wei, S. Manolidis, J. T. Roland Jr, and N. Simaan, "Path planning and workspace determination for robot-assisted insertion of steerable electrode arrays for cochlear implant surgery," in *30th Annual International Conference of the IEEE Medical Image Computing and Computer-Assisted Intervention (MICCAI)*. Springer, 2008, pp. 692–700.
- [76] B. Bell, C. Stieger, N. Gerber, A. Arnold, C. Nauer, V. Hamacher, M. Kompis, L. Nolte, M. Caversaccio, and S. Weber, "A self-developed and constructed robot for minimally invasive cochlear implantation," *Acta oto-laryngologica*, vol. 132, no. 4, pp. 355–360, 2012.
- [77] T. M. Williamson, B. J. Bell, N. Gerber, L. Salas, P. Zysset, M. Caversaccio, and S. Weber, "Estimation of tool pose based on force–density correlation during robotic drilling," *IEEE Transactions on Biomedical Engineering*, vol. 60, no. 4, pp. 969–976, 2013.
- [78] J. Ansó, C. Stahl, N. Gerber, T. Williamson, K. Gavaghan, K. M. Rösler, M.-D. Caversaccio, S. Weber, and B. Bell, "Feasibility of using emg for early detection of the facial nerve during robotic direct cochlear access," *Otology & Neurotology*, vol. 35, no. 3, pp. 545–554, 2014.
- [79] B. Bell, N. Gerber, T. Williamson, K. Gavaghan, W. Wimmer, M. Caversaccio, and S. Weber, "In vitro accuracy evaluation of image-guided robot system for direct cochlear access," *Otology & Neurotology*, vol. 34, no. 7, pp. 1284–1290, 2013.
- [80] Y. Zhang, T. Pfeiffer, M. Weller, W. Wieser, R. Huber, J. Raczkowski, J. Schipper, H. Wörn, and T. Klenzner, "Optical coherence tomography guided laser cochleostomy: Towards the accuracy on tens of micrometer scale," *BioMed research international*, vol. 2014, 2014.
- [81] Y. Zhang and H. Worn, "Optical coherence tomography as highly accurate optical tracking system," in *2014 IEEE/ASME International Conference on Advanced Intelligent Mechatronics (AIM)*. IEEE, 2014, pp. 1145–1150.
- [82] Y. Zhang and H. Worn, "Optical coherence tomography as highly accurate optical tracking system," in *2014 IEEE/ASME International Conference on Advanced Intelligent Mechatronics (AIM)*. IEEE, 2014, pp. 1145–1150.
- [83] R. F. Labadie, J. Mitchell, R. Balachandran, and J. M. Fitzpatrick, "Customized, rapid-production microstereotactic table for surgical targeting: description of concept and in vitro validation," *International journal of computer assisted radiology and surgery*, vol. 4, no. 3, pp. 273–280, 2009.
- [84] L. B. Kratchman, G. S. Blachon, T. J. Withrow, R. Balachandran, R. F. Labadie, and R. J. Webster, "Design of a bone-attached parallel robot for percutaneous cochlear implantation," *IEEE Transactions on Biomedical Engineering*, vol. 58, no. 10, pp. 2904–2910, 2011.

- [85] A. Danilchenko, R. Balachandran, J. L. Toennies, S. Baron, B. Munske, J. M. Fitzpatrick, T. J. Withrow, R. J. Webster III, and R. F. Labadie, “Robotic mastoidectomy,” *Otology & neurotology: official publication of the American Otological Society, American Neurotology Society [and] European Academy of Otology and Neurotology*, vol. 32, no. 1, pp. 11–16, 2011.
- [86] N. P. Dillon, R. Balachandran, A. M. dit Falisse, G. B. Wanna, R. F. Labadie, T. J. Withrow, J. M. Fitzpatrick, and R. J. Webster, “Preliminary testing of a compact bone-attached robot for otologic surgery,” in *SPIE Medical Imaging*, vol. 9036. International Society for Optics and Photonics, 2014.
- [87] J. H. Noble, F. M. Warren, R. F. Labadie, and B. M. Dawant, “Automatic segmentation of the facial nerve and chorda tympani in ct images using spatially dependent feature values,” *Medical physics*, vol. 35, no. 12, pp. 5375–5384, 2008.
- [88] J. H. Noble, B. M. Dawant, F. M. Warren, and R. F. Labadie, “Automatic identification and 3-d rendering of temporal bone anatomy,” *Otology & neurotology: official publication of the American Otological Society, American Neurotology Society [and] European Academy of Otology and Neurotology*, vol. 30, no. 4, p. 436, 2009.
- [89] H. Lim, J.-M. Han, J. Hong, B.-J. Yi, S. H. Lee, J. H. Jeong, N. Matsumoto, M. Oka, S. Komune, and M. Hashizume, “Image-guided robotic mastoidectomy using human-robot collaboration control,” in *International Conference on Mechatronics and Automation (ICMA)*, 2011, pp. 549–554.
- [90] M. Miroir, Y. Nguyen, J. Szewczyk, S. Mazalaigue, E. Ferrary, O. Sterkers, and A. B. Grayeli, “Robotol: from design to evaluation of a robot for middle ear surgery,” in *IEEE/RSJ International Conference on Intelligent Robots and Systems (IROS)*, 2010, pp. 850–856.
- [91] M. Miroir, J. Szewczyk, Y. Nguyen, S. Mazalaigue, and O. Sterkers, “Design of a robotic system for minimally invasive surgery of the middle ear,” in *2nd IEEE RAS & EMBS International Conference on Biomedical Robotics and Biomechanics (BioRob)*, 2008, pp. 747–752.
- [92] Y. Nguyen, M. Miroir, G. Kazmitcheff, E. Ferrary, O. Sterkers, and A. B. Grayeli, “From conception to application of a tele-operated assistance robot for middle ear surgery,” *Surgical innovation*, vol. 19, no. 3, pp. 241–251, 2012.
- [93] T. Maier, G. Strauss, M. Hofer, T. Kraus, A. Runge, R. Stenzel, J. Gumprecht, T. Berger, A. Dietz, and T. C. Lueth, “A new micromanipulator system for middle ear surgery,” in *IEEE International Conference on Robotics and Automation (ICRA)*, 2010, pp. 1568–1573.
- [94] T. Maier, G. Strauss, F. Bauer, A. Grasser, N. Hata, and T. C. Lueth, “Distance measurement in middle ear surgery using a telemanipulator,” in *Medical Image Computing and Computer-Assisted Intervention–MICCAI*. Springer, 2011, pp. 41–48.
- [95] K. Entsfellner, R. Tauber, D. B. Roppenecker, J. D. Gumprecht, G. Strauss, and T. Lueth, “Development of universal gripping adapters: Sterile coupling of medical devices and robots using robotic fingers,” in *IEEE/ASME International Conference on Advanced Intelligent Mechatronics (AIM)*, 2013, pp. 1464–1469.
- [96] K. C. Olds, P. Chalasani, P. Pacheco-Lopez, I. Iordachita, L. M. Akst, and R. H. Taylor, “Preliminary evaluation of a new microsurgical robotic system for head and neck surgery,” in *IEEE/RSJ International Conference on Intelligent Robots and Systems (IROS)*, 2014, pp. 1276–1281.
- [97] L. Fichera, N. P. Dillon, D. Zhang, I. S. Godage, M. A. Siebold, B. I. Hartley, J. H. Noble, P. T. Russell, R. F. Labadie, and R. J. Webster, “Through the eustachian tube and beyond: A new miniature robotic endoscope to see into the middle ear,” *IEEE Robotics and Automation Letters*, vol. 2, no. 3, pp. 1488–1494, 2017.

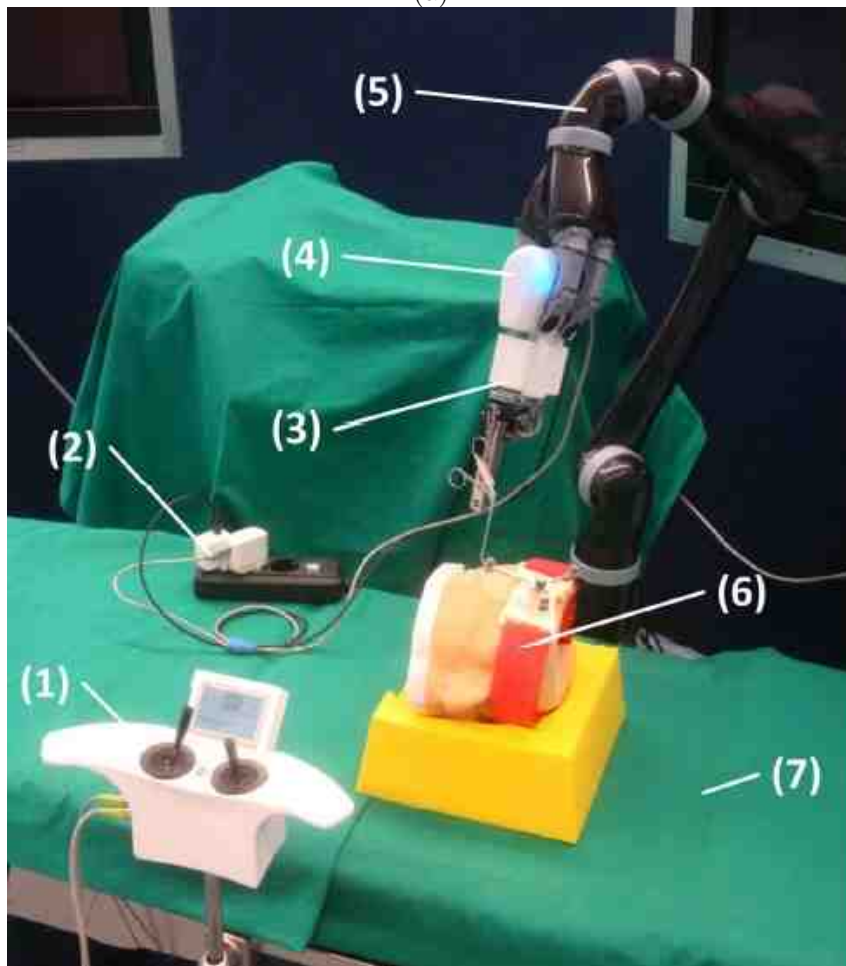
- [98] X. He, V. van Geirt, P. Gehlbach, R. Taylor, and I. Iordachita, “Iris: Integrated robotic intraocular snake,” in IEEE International Conference on Robotics and Automation (ICRA), 2015, pp. 1764–1769.
- [99] P. A. York, P. J. Swaney, H. B. Gilbert, and R. J. Webster, “A wrist for needle-sized surgical robots,” in IEEE International Conference on Robotics and Automation (ICRA)., 2015, pp. 1776–1781.
- [100] R. J. Webster and B. A. Jones, “Design and kinematic modeling of constant curvature continuum robots: A review,” *The International Journal of Robotics Research*, 2010.
- [101] I. D. Walker, “Continuous backbone “continuum” robot manipulators,” *ISRN Robotics*, vol. 2013, 2013.
- [102] J. Burgner-Kahrs, D. C. Rucker, and H. Choset, “Continuum robots for medical applications: A survey,” *IEEE Transactions on Robotics*, vol. 31, no. 6, pp. 1261–1280, 2015.
- [103] C. Betz, V. Volgger, S. Silverman, M. Rubinstein, M. Kraft, C. Arens, and B. Wong, “Clinical optical coherence tomography in head and neck oncology: overview and outlook,” *Head Neck Oncol*, vol. 5, no. 3, p. 35, 2013.
- [104] B. Davies, “A review of robotics in surgery,” *Proceedings of the Institution of Mechanical Engineers, Part H: Journal of Engineering in Medicine*, vol. 214, no. 1, pp. 129–140, 2000.
- [105] R. H. Taylor and D. Stoianovici, “Medical robotics in computer-integrated surgery,” *IEEE Transactions on Robotics and Automation*, vol. 19, no. 5, pp. 765–781, 2003.
- [106] P. P. Pott, H.-P. Scharf, and M. L. Schwarz, “Today’s state of the art in surgical robotics,” *Computer Aided Surgery*, vol. 10, no. 2, pp. 101–132, 2005.
- [107] G. Dogangil, B. Davies, and F. R. y Baena, “A review of medical robotics for minimally invasive soft tissue surgery,” *Proceedings of the Institution of Mechanical Engineers, Part H: Journal of Engineering in Medicine*, vol. 224, no. 5, pp. 653–679, 2009.
- [108] C.-H. Kuo, J. S. Dai, and P. Dasgupta, “Kinematic design considerations for minimally invasive surgical robots: an overview,” *The International Journal of Medical Robotics and Computer Assisted Surgery*, vol. 8, no. 2, pp. 127–145, 2012.
- [109] B. Dahroug, B. Tamadazte, and N. Andreff, “3d path following with remote center of motion constraints,” in *13th International Conference on Informatics in Control, Automation and Robotics (ICINCO).*, vol. 1, 2016, pp. 84–91.
- [110] B. Maurin, O. Piccin, B. Bayle, J. Gangloff, M. de Mathelin, L. Soler, and A. Gangi, “A new robotic system for ct-guided percutaneous procedures with haptic feedback,” in *International Congress Series*, vol. 1268. Elsevier, 2004, pp. 515–520.
- [111] T. Greigarn and M. C. Çavuşoğlu, “Task-space motion planning of mri-actuated catheters for catheter ablation of atrial fibrillation,” in *IEEE/RSJ International Conference on Intelligent Robots and Systems (IROS)*, 2014, pp. 3476–3482.
- [112] M.-A. Vitrani, G. Morel, and T. Ortmaier, “Automatic guidance of a surgical instrument with ultrasound based visual servoing,” in *Proceedings of the 2005 IEEE International Conference on Robotics and Automation (ICRA).*, 2005, pp. 508–513.
- [113] B. Dahroug, B. Tamadazte, and N. Andreff, “Visual servoing controller for time-invariant 3d path following with remote centre of motion constraint,” in *IEEE International Conference on Robotics and Automation (ICRA)*, 2017.
- [114] N. Nathoo, M. C. Çavusoglu, M. A. Vogelbaum, and G. H. Barnett, “In touch with robotics: neurosurgery for the future,” *Neurosurgery*, vol. 56, no. 3, pp. 421–433, 2005.

- [115] J. Kettenbach, G. Kronreif, A. Melzer, G. Fichtinger, D. Stoianovici, and K. Cleary, "Ultrasound-, ct-and mr-guided robot-assisted interventions," in *Image Processing in Radiology*. Springer, 2008, pp. 393–409.
- [116] B. Fei, W. S. Ng, S. Chauhan, and C. K. Kwok, "The safety issues of medical robotics," *Reliability Engineering & System Safety*, vol. 73, no. 2, pp. 183–192, 2001.
- [117] W. Korb, M. Kornfeld, W. Birkfellner, R. Boesecke, M. Figl, M. Fuerst, J. Kettenbach, A. Vogler, S. Hassfeld, and G. Kornreif, "Risk analysis and safety assessment in surgical robotics: A case study on a biopsy robot," *Minimally Invasive Therapy & Allied Technologies*, vol. 14, no. 1, pp. 23–31, 2005.
- [118] N. Simaan, R. Taylor, and P. Flint, "A dexterous system for laryngeal surgery," in *IEEE International Conference on Robotics and Automation (ICRA)*., vol. 1, 2004, pp. 351–357.
- [119] J. M. Jani, M. Leary, A. Subic, and M. A. Gibson, "A review of shape memory alloy research, applications and opportunities," *Materials & Design*, vol. 56, pp. 1078–1113, 2014.
- [120] T. Shoa, J. D. Madden, N. Fekri, N. R. Munce, and V. X. Yang, "Conducting polymer based active catheter for minimally invasive interventions inside arteries," in *30th Annual International Conference of the IEEE Engineering in Medicine and Biology Society (EMBS)*., 2008, pp. 2063–2066.
- [121] M. T. Chikhaoui, A. Cot, K. Rabenorosoa, P. Rougeot, and N. Andreff, "Design and closed-loop control of a tri-layer polypyrrole based telescopic soft robot," in *IEEE/RSJ International Conference on Intelligent Robots and Systems (IROS)*, 2016, pp. 1145–1150.





(a)



(b)

Fig. 19. (a) Master-slave MMS-II surgical system with forceps tool [93]; (b) master-slave MMTS surgical system, where (1) joystick console, (2) energy supply, (3) MMS, (4) active gripping adapter, (5) carrier robot, (6) patient phantom, (7) OR-table.

Robot data

- Macro-manipulator:
  - large workspace  
(around  $1000mm \times 1000mm \times 500mm$ ),
  - range (around  $500mm$ ),
- bendable micro-end-effector:
  - actuation type (tendon-driven, smart material or magnetic field),
  - small workspace (around  $5 \times 15 \times 15mm^3$ , Fig. 21),
  - range ( $15mm$ ),
  - number of segments (2),
  - hollow segments,
  - outer diameter ( $0.5 - 2mm$  [47] [97]),
  - length ( $> 30mm$  [76] [97]),
  - bending radius ( $< 3mm$ ),
  - bending angle ( $\geq 90^\circ$  [97]),
  - resolution ( $< 0.02mm$  [90]),
  - force ( $< 5N$  [90]),
  - payload (few grams)
- Modelling and control
  - adaptability to patient variability and safety
  - accuracy (100% of the above characteristics) and response time ( $< 0.1$  second)
- Fabrication
  - bio-compatibility, environmentally friendly and low cost

TABLE III

Summary of the robot data.

CAS data

- exteroceptive sensors
  - optical tracking with accuracy (around  $0.05mm$  <sup>12</sup>)
  - micro-fiber-optic imaging probe:
    - \* resolution ( $< 10m$  Fig. 20),
    - \* depth ( $> 1mm$ ),
    - \* FOV (around  $90^\circ$  [97]),
    - \* frequency of image acquisition (around  $30Hz$  [97])
- Pre-operative planning software
  - segmentation: yes (semi or fully automated),
  - 3D reconstruction of anatomical structures: yes,
  - registration: accuracy ( $< 0.2mm$  [63]),
  - access tunnel and ablation path planning: yes
- Intra-operative control software
  - real-time navigation control
- Surgeon-robot interface: interface software, simulator, co-manipulation (hand tremor, semi-automated), fully automated, virtual reality and learning

TABLE IV  
Summary of CAS data.

Risk analysis (risk level, risk impact)

- robot structure
  - access to some anatomical locations may be infeasible due to insufficient DOF of the micro-robotic tool (low level, medium impact)
  - the required bending angle or radius of curvature is very high to reach the entire workspace (low level, medium impact)
  - pull out the robot from the patient body in case of system failure without damaging critical structures (low level, high impact)
- CAS software
  - critical structures are not visible in available image data due to factors such as insufficient contrast or spatial resolution (medium level, medium impact)
  - unable to plan a safe trajectory due to space between critical anatomy with the required drill diameter (low level, high impact)
  - accuracy of the robotic system is insufficient (low level, high impact)
  - insufficient image quality for accurate image guidance (medium level, high impact)

TABLE V

Primary risk analysis.

TABLE VI

Summary of surgical robotic systems. The abbreviations stand for: Kinematic structure (Serial/Parallel/Special Structure), Actuation source (Passive/Active), Rigid tool (Straight/Curved), Bendable tool (Continuous/Discrete), Actuation type (Magnetic/Cable-Driven/Concentric Tube), Tool type (Driller/Forces/Electrode/Laser), Proprioceptive sensor (Joint Sensors/Force Sensor), Extroceptive sensor (Stereo-Camera/Endoscope/Standard Otomicroscope), Degree of Autonomy (Co-Operative/Semi Automated/Fully Automated)

No.	Previous works	Applications	Status	Robot structure									CAS software			Tool type	Proprioceptive sensor	Extroceptive sensor	Degree of Autonomy	
				Robot's manipulator			Robot's end-effector						Tool exchanger	Segmentation	Planning					Navigation
				Kinematic structure	Degree of freedom	Actuation source	Rigid tool	Bendable tool	Number of Sections	Degree of freedom	Actuation type									
1	[68]	Stapedectomy	Prototype	-	-	-	S	-	-	-	-	-	-	-	-	√	D	FS	-	CO
2	[61]	Stapedectomy	Prototype	-	-	-	S	-	-	-	-	-	-	-	-	√	D	FS	-	CO
3	[66]	Cochleostomy	Prototype	S	-	P	S	-	-	-	-	-	-	-	-	√	D	FS	-	FA
4	[67]	Cochleostomy	Prototype	S/P	6	A	S	-	-	-	-	-	√	-	√	√	D	-	-	SA
5	(Hannover Univ., Germany) [73]	Cochleostomy	Prototype	S	6	A	-	-	-	-	-	-	√	√	√	√	D/E	-	CT/SC	SA
6	Microtable (Vanderbilt Univ., USA) [84]	Cochleostomy	Prototype	P	6	A	-	-	-	-	-	-	√	√	√	√	D/E	-	CT	SA
7	Otobot (Vanderbilt Univ., USA) [85]	Mastoidectomy	Prototype	S	6	A	S	-	-	-	-	-	√	√	√	√	D	-	CT/SC	SA
8	(Hanyang Univ., South Korea) [89]	Mastoidectomy	Prototype	SS	5	A	S	-	-	-	-	-	√	√	√	√	D	-	CT/SC	CO
9	MMS (TUM, Germany) [94]	Stapedectomy	Prototype	S	4	P	S	-	-	-	-	-	-	-	-	-	D/F/E	FS	-	CO
10	RobOtol (IRIS, France) [92]	Stapedectomy	Experimental	SS	6	A	S	-	-	-	-	-	-	-	-	-	D/F	-	SO	CO
11	[64]	Cochleostomy	Prototype	-	-	-	-	C	1	2	M	-	-	-	-	√	E	FS	-	SA
12	MMTS (TUM, Germany) [95]	Stapedectomy	Prototype	S	6	A	S	-	-	-	-	-	-	-	-	-	D/F	-	-	CO
13	[65]	Cochleostomy	Prototype	P	6	A	-	-	-	-	-	-	-	-	-	√	E	FS	-	SA
14	(Vanderbilt Univ., USA) [86]	Mastoidectomy	Prototype	P	6	A	S	-	-	-	-	-	√	√	√	√	D	-	CT	SA
15	(KIT, Germany) [82]	Cochleostomy	Prototype	-	-	P	-	-	-	-	-	-	-	-	-	√	L	-	OCT	SA
16	Da Vinci (JHU, USA) [69]	Mastoidectomy electrode insertion	Experimental	S	-	A	-	-	-	-	-	-	√	√	√	√	D/E	JS/FS	CT/E	CO
17	(ARTORG, Swiss) [63]	Cochleostomy	Experimental	S	5	A	S	-	-	-	-	-	√	√	√	√	D	JS/FS	CT/SC	SA
18	(Vanderbilt Univ., USA) [97]	Cholesteatoma	Prototype	-	-	-	-	C	1	3	CD	-	-	-	-	√	-	-	E	FA